deficiency is linked to a genetic defect in the phospholipase gene LIPH. Science 314:982–985.

Kljuic A, Bazzi H, Sundberg JP, Martinez-Mir A, O'Shaughnessy R, Mahoney MG, Levy M, Montagutelli X, Ahmad W, Aita VM, Gordon D, Uitto J, Whiting D, Ott J, Fischer S, Gilliam TC, Jahoda CA, Morris RJ, Panteleyev AA, Nguyen VT, Christiano AM. 2003. Desmoglein 4 in hair follicle differentiation and epidermal adhesion: evidence from inherited hypotrichosis and acquired pemphigus vulgaris. Cell 113:249–260.

Kubiak RJ, Yue X, Hondal RJ, Mihai C, Tsai MD, Bruzik KS. 2001. Involvement of the Arg-Asp-His catalytic triad in enzymatic cleavage of the phosphodiester bond. Biochemistry 40:5422–5432.

Moss C, Martinez-Mir A, Lam H, Tadin-Strapps M, Kljuic A, Christiano AM. 2004. A recurrent intragenic deletion in the desmoglein 4 gene underlies localized autosomal recessive hypotrichosis. J Invest Dermatol 123:607–610.

Nahum S, Pasternack SM, Pforr J, Indelman M, Wollnik B, Bergman R, Nothen MM, Konig A, Khamaysi Z, Betz RC, Sprecher E. 2009. A large duplication in LIPH underlies autosomal recessive hypotrichosis simplex in four Middle Eastern families. Arch Dermatol Res 301:391–393.

Naz G, Khan B, Ali G, Azeem Z, Wali A, Ansar M, Ahmad W. 2009. Novel missense mutations in lipase H (LIPH) gene causing autosomal recessive hypotrichosis (LAH2). J Dermatol Sci 54:12–16.

Ohtsu H, Dempsey PJ, Eguchi S. 2006. ADAMs as mediators of EGF receptor transactivation by G protein-coupled receptors. Am J Physiol Cell Physiol 291:C1–C10.

Pasternack SM, von Kugelgen I, Aboud KA, Lee YA, Ruschendorf F, Voss K, Hillmer AM, Molderings GJ, Franz T, Ramirez A, Nürnberg P, Nöthen MM, Betz RC. 2008. G protein-coupled receptor P2Y5 and its ligand LPA are involved in maintenance of human hair growth. Nat Genet 40:329–334.

Pasternack SM, von Kugelgen I, Muller M, Oji V, Traupe H, Sprecher E, Nothen MM, Janecke AR, Betz RC. 2009. In vitro analysis of LIPH mutations causing hypotrichosis simplex: evidence confirming the role of lipase H and lysophosphatidic acid in hair growth. J Invest Dermatol 129:2772–2776.

Petukhova L, Shimomura Y, Wajid M, Gorroochurn P, Hodge SE, Christiano AM. 2009. The effect of inbreeding on the distribution of compound heterozygotes: a lesson from Lipase H mutations in autosomal recessive woolly hair/hypotrichosis. Hum Hered 68:117–130.

Rafique MA, Ansar M, Jamal SM, Malik S, Sohail M, Faiyaz-Ul-Haque M, Haque S, Leal SM, Ahmad W. 2003. A locus for hereditary hypotrichosis localized to human chromosome 18q21.1. Eur J Hum Genet 11: 623–628.

Shimomura Y, Ito M, Christiano AM. 2009a. Mutations in the LIPH gene in three Japanese families with autosomal recessive woolly hair/hypotrichosis. J Dermatol Sci 56:205–207.

Shimomura Y, Wajid M, Ishii Y, Shapiro L, Petukhova L, Gordon D, Christiano AM. 2008. Disruption of P2RY5, an orphan G protein-coupled receptor, underlies autosomal recessive woolly hair. Nat Genet 40:335–339.

Shimomura Y, Wajid M, Petukhova L, Shapiro L, Christiano AM. 2009b. Mutations in the lipase H gene underlie autosomal recessive woolly hair/hypotrichosis. J Invest Dermatol 129:622–628.

Shimomura Y, Wajid M, Zlotogorski A, Lee YJ, Rice RH, Christiano AM. 2009c. Founder mutations in the lipase h gene in families with autosomal recessive woolly hair/hypotrichosis. J Invest Dermatol 129:1927–1934.

Sonoda H, Aoki J, Hiramatsu T, Ishida M, Bandoh K, Nagai Y, Taguchi R, Inoue K, Arai H. 2002. A novel phosphatidic acid-selective phospholipase A1 that produces lysophosphatidic acid. J Biol Chem 277:34254–34263.

Tokumaru S, Higashiyama S, Endo T, Nakagawa T, Miyagawa JI, Yamamori K, Hanakawa Y, Ohmoto H, Yoshino K, Shirakata Y, Matsuzawa Y, Hashimoto K, Taniguchi N. 2000. Ectodomain shedding of epidermal growth factor receptor ligands is required for keratinocyte migration in cutaneous wound healing. J Cell Biol 151:209–220.

Wali A, Chishti MS, Ayub M, Yasinzai M, Kafaitullah, Ali G, John P, Ahmad W. 2007. Localization of a novel autosomal recessive hypotrichosis locus (LAH3) to chromosome 13q14.11–q21.32. Clin Genet 72:23–29.

Whittock NV, Bower C. 2003. Genetic evidence for a novel human desmosomal cadherin, desmoglein 4. J Invest Dermatol 120:523–530.

Xu X, Quiros RM, Gattuso P, Ain KB, Prinz RA. 2003. High prevalence of BRAF gene mutation in papillary thyroid carcinomas and thyroid tumor cell lines. Cancer Res 63:4561–4567.

The American Journal of Pathology, Vol. 177, No. 1, July 2010

DOI: 10.2353/ajpath.2010.091120

Epithelial and Mesenchymal Cell Biology

Self-Improvement of Keratinocyte Differentiation Defects During Skin Maturation in ABCA12-Deficient Harlequin Ichthyosis Model Mice

Teruki Yanagi,* Masashi Akiyama,* Hiroshi Nishihara,† Junko Ishikawa,‡ Kaori Sakai,* Yuki Miyamura,* Ayano Naoe,‡ Takashi Kitahara,‡ Shinya Tanaka,§ and Hiroshi Shimizu*

From the Department of Dermatology, Laboratory of Translational Pathology,† the Laboratory of Cancer Research,§ the Department of Pathology, Hokkaido University Graduate School of Medicine, Sapporo; and Tochigi Research Laboratories,‡ Kao Corporation, Ichikai, Haga, Tochigi, Japan*

Harlequin ichthyosis (HI) is caused by loss-of-function mutations in the keratinocyte lipid transporter ABCA12. The patients often die in the first 1 or 2 weeks of life, although HI survivors' phenotypes improve within several weeks after birth. In order to clarify the mechanisms of phenotypic recovery, we studied grafted skin and keratinocytes from *Abca12*-disrupted (*Abca12*$^{-/-}$) mice showing abnormal lipid transport. *Abca12*$^{-/-}$ neonatal epidermis showed significantly reduced total ceramide amounts and aberrant ceramide composition. Immunofluorescence and immunoblotting of *Abca12*$^{-/-}$ neonatal epidermis revealed defective profilaggrin/filaggrin conversion and reduced protein expression of the differentiation-specific molecules, loricrin, kallikrein 5, and transglutaminase 1, although their mRNA expression was up-regulated. In contrast, *Abca12*$^{-/-}$ skin grafts kept in a dry environment exhibited dramatic improvements in all these abnormalities. Increased transepidermal water loss, a parameter representing barrier defect, was remarkably decreased in grafted *Abca12*$^{-/-}$ skin. Ten-passage sub-cultured *Abca12*$^{-/-}$ keratinocytes showed restoration of intact ceramide distribution, differentiation-specific protein expression and profilaggrin/filaggrin conversion, which were defective in primary-cultures. Using cDNA microarray analysis, lipid transporters including four ATP-binding cassette transporters were up-regulated after sub-culture of *Abca12*$^{-/-}$ keratinocytes compared with primary-culture. These results indicate that disrupted keratinocyte differentiation during the fetal development is involved in the pathomechanism of HI and, during maturation, *Abca12*$^{-/-}$ epidermal keratinocytes regain normal differentiation processes. This restoration may account for the skin phenotype improvement observed in HI survivors. *(Am J Pathol 2010, 177:106–118; DOI: 10.2353/ajpath.2010.091120)*

Harlequin ichthyosis (HI) (OMIM 242500) is one of the most severe genetic skin disorders, and its clinical features at birth include severe ectropion, eclabium, flattening of the ears, and large thick plate-like scales over the entire body.[1] Infants affected with HI frequently die within the early neonatal period, although an increasing survival rate for HI newborns has recently been highlighted.[2] In 2005, we and another independent research group identified mutations in the ATP-binding cassette transporter A12 (ABCA12) gene as the cause of HI.[3,4] We previously demonstrated that a severe ABCA12 deficiency causes defective lipid transport in lamellar granules in the upper spinous and granular layer keratinocytes, resulting in malformation of intercellular lipid layers at the granular/cornified layer interface and epidermal lipid barrier disruption resulting in HI phenotype.[3] We recently generated *Abca12*-disrupted (*Abca12*$^{-/-}$) mice by targeting *Abca12*, which closely reproduced the human HI phenotype and died soon after birth.[5] We tried systemic retinoid administration to the pregnant female mice as a form of fetal therapy, although no therapeutic effect was

Supported in part by a grant-in-aid from the Ministry of Education, Science, Sports, and Culture of Japan (Kiban B 20390304: to M.A.), a grant from Ministry of Health, Labor and Welfare of Japan (Health and Labor Sciences Research grants; Research on Intractable Disease: H21–047 and H22-177: to M.A.), a grant from ONO Medical Research Foundation (T.Y.) and a grant from Kanae Foundation for the promotion of Medical Science (T.Y.).

Accepted for publication February 26, 2010.

None of the authors declare any relevant financial relationships.

Supplemental material for this article can be found on *http://ajp.amjpathol.org*.

Address reprint requests to Masashi Akiyama, M.D., Ph.D., or Hiroshi Shimizu, M.D., Ph.D., Department of Dermatology, Hokkaido University Graduate School of Medicine, N15 W7, Kita-ku, Sapporo 060-8638, Japan. E-mail: akiyama@med.hokudai.ac.jp or shimizu@med.hokudai.ac.jp.

obtained in the *Abca12*$^{-/-}$ newborns after treatment.[5] After our publication, Zuo et al[6] also reported another *Abca12* knockout mouse, whose skin showed similar features to our model mice.

Previously, we demonstrated severe skin barrier defects in *Abca12*$^{-/-}$ mice and suggested that "barrier insufficiency" plays an important role in HI phenotype expression.[5] However, "the barrier insufficiency" theory fails to completely explain the pathomechanism of the HI phenotype. HI fetuses show a HI phenotype even *in utero*, where skin barrier protection against a dry environment is not required. In addition, the skin phenotype of HI long-term survivors maintained in a dry environment shows a dramatic improvement within several weeks after birth where they require a normal skin barrier function. Thus, we suspected that other unknown mechanisms are involved in HI and the formation HI survivors' skin phenotypes. To date there have been no reports which have compared the skin phenotypes in fatally affected HI neonates and survivors, and the exact mechanism of HI survivors' skin phenotype improvement has yet to be clarified. Thus, we have carefully analyzed the keratinization process of neonatal versus grafted HI model mice skin and primary versus subcultured *Abca12*$^{-/-}$ keratinocytes instead of human HI neonatal and survivors' skin. Initially, we investigated the distribution and amounts/composition of lipids, and expression of differentiation-specific molecules in neonatal HI model mice skin. Then, we studied the alteration of them in grafted HI model mouse skin transplanted onto severe combined immunodeficient (SCID) mice. In addition, we performed keratinocyte culture experiments including immunostaining and Western blotting using primary/subcultured *Abca12*$^{-/-}$ keratinocytes to confirm the results of the neonatal and grafted skin experiments. Further, we analyzed the whole gene expression profile of primary versus subcultured *Abca12*$^{-/-}$ keratinocytes using cDNA microarray methods. Finally, we conducted therapeutic trials on primary-cultured *Abca12*$^{-/-}$ keratinocytes and grafted HI model mice skin with retinoids.

Materials and Methods

Animals

All animal studies were reviewed and approved by the Animal Use and Care Committee of the Hokkaido University Graduate School of Medicine. C57BL/6 strain mice and SCID mice were purchased from Clea (Tokyo, Japan). All animals used for this study were maintained under pathogen-free conditions.

Antibodies

Rabbit polyclonal affinity purified anti-mouse Abca12 antibody was raised in rabbits using a 14-amino acid sequence synthetic peptide (residues 2581 to 2594) derived from the mouse Abca12 sequence (XM001002308) as the immunogen.[5] The other primary antibodies were rabbit anti-profilaggrin/filaggrin antibody (COVANCE, Princeton, NJ), rabbit anti-involucrin antibody (M-116; Santa Cruz Biotechnology, Santa Cruz, CA), rabbit anti-desmoglein 1 antibody (H-290; Santa Cruz Biotechnology), rabbit anti-mouse loricrin antibody (AF62; COVANCE), rabbit anti-kallikrein 5 antibody (ab7283; Abcam, Cambridge, UK), rabbit anti-glucosylceramide/ceramide antibody (Glycobiotech, Kukels, Germany), and mouse monoclonal anti-β actin antibody (Sigma Chemical Co., St. Louis, MO). Secondary antibodies used in the present study were as follows; Alexa Fluor 488-conjugated donkey anti-rabbit IgG (Invitrogen Corp., Carlsbad, CA), fluorescein isothiocyanate-conjugated goat anti-rabbit IgG (Jackson Immuno Research, West Grove, PA), horseradish peroxidase-conjugated goat anti-rabbit IgG or horseradish peroxidase-conjugated goat anti-mouse IgG (Invitrogen Corp.).

Generation of Abca12$^{-/-}$ *Mouse*

The procedure for generating *Abca12*$^{-/-}$ mice has been previously described.[5] Briefly, we cloned mouse genomic DNA Abca12 fragments from the mouse 129Sv/Ev genomic library (Bacpac Resources Center, Children's Hospital Oakland Research Institute, Oakland, CA). We subcloned a 10.6-kb fragment to make the targeting vector. We inserted the PGK/Neo cassette between 47 bp upstream of the exon 30 and 203 bp downstream of exon 30. We transfected the targeting vector by electroporation into 129Sv/Ev embryonic stem cells, then microinjected the correctly targeted embryonic stem cell line into blastocysts obtained from C57BL/6 mice to generate chimeric mice, which we then mated with C57BL/6 females. We crossed the heterozygotes with C57BL/6 over at least five generations, and then intercrossed them to generate the *Abca12*$^{-/-}$ mice. Genotyping was performed by PCR as described previously.[5]

Establishment of Abca12$^{-/-}$ *Mice Keratinocyte Culture*

Skin samples from *Abca12*$^{-/-}$ and wild-type mice were processed for primary keratinocyte culture, and cells were grown according to standard procedures in CnT-57 medium (Cellntec Advanced Cell Systems, Bern, Switzerland). For differentiation induction, culture medium was switched from CnT-57 medium to CnT-02 medium (Cellntec Advanced Cell Systems) and, 24 hours later, the calcium concentration was changed to 1.2 mmol/L. 48 hours later, we performed extractions of total RNA and protein from cultured cells. We established primary-cultured keratinocytes from two *Abca12*$^{-/-}$ mice and two wild-type mice.

Skin Grafting

In total, ten *Abca12*$^{-/-}$ and three wild-type neonates were sacrificed by anesthesia with ether inhalation, and their dorsal skin excised and transplanted onto SCID mice (Clea). Those skin grafts were fully adapted within 2 weeks after grafting. At 3 weeks after transplantation, the skin grafts were harvested for further analysis.

Extraction of Total RNA and Real-Time Reverse Transcriptase PCR Analysis

We separated the epidermis from whole skin samples of wild and *Abca12−/−* mice by 1 mol/L NaCl in sterile water at 4°C for 2 hours. We isolated total RNA from the epidermis using the Quick Gene RNA Tissue Kit SII (Fujifilm Corp, Tokyo, Japan). We also isolated total RNA from keratinocytes cultured from wild-type and *Abca12−/−* skin using the RNeasy mini kit (Qiagen Corp, Tokyo, Japan). RNA concentration was measured spectrophotometrically and samples were stored at −80°C until use for reverse transcriptase PCR. We reverse-transcribed RNA using Superscript II (Invitrogen Corp.) following the manufacturer's instructions. Complementary DNA samples were analyzed by ABI prism 7000 sequence detection system (Applied Biosystems, Foster City, CA). Primers and probes specific for differentiation-specific protein genes including loricrin, kallikrein 5, transglutaminase 1, involucrin, filaggrin, and control house keeping genes, glyceraldehyde-3-phosphate dehydrogenase (GAPDH), and β-actin, were obtained from Taqman Gene Expression Assay (Applied Biosystems) (Probe ID; Mm01962650_s1, Mm01203811_a1, Mm00498375_a1, Mm00515219_s1, Mm01716522_m1, Mm99999915_g1, and Mm00607939_s1). Differences between the mean CT values of loricrin, kallikrein 5, transglutaminase 1, involucrin, filaggrin and those of GAPDH or β-actin were calculated as: ΔCT*Abca12−/−* mice = CTloricrin (or other keratinization markers) − CTGAPDH (or other house keeping genes) and those of ΔCT for the *Abca12+/+* asΔCT calibrator = CTloricrin (or other keratinization markers) − CTGAPDH (or other house keeping genes).

We could obtain the similar results from GAPDH and β-actin standard, thus we described the results of GAPDH standard in the present study. Final results for *Abca12*$^{-/-}$ mouse samples/wild-type mouse samples (%) were determined by $2^{-(}$ΔCTAbca12−/− sample − ΔCTcalibrator). We measured mRNA levels five times for each clones. Using similar methods, we quantitatively analyzed these differentiation-specific mRNA expression levels in the primary/subcultured keratinocytes from *Abca12*$^{-/-}$ and wild-type mice.

Western Blotting

We separated the epidermis from whole skin samples of wild and *Abca12*$^{-/-}$ mice by 1mol/L NaCl in sterile water at 4°C for 2 hours. For Western blotting, we used epidermal homogenates and proteins extracted from cultured keratinocytes prepared with radioimmunoprecipitation assay (RIPA) buffer comprising 50 mmol/L Tris-HCl, pH7.5, 150 mmol/L NaCl, 1% Nonidet P-40, 0.5% deoxycholate, 0.1% SDS, and Roche protease cocktail tablet (Roche, Basel, Switzerland). Protein concentrations were measured using Micro BCA protein assay kit (Thermo Scientific, Rockford, IL). Protein concentration of the samples for western blotting was from 1 to 2 μg/μl. The 20 μg protein loading per single lane was separated by a 5 to 20% gradient gel SDS-polyacrylamide gel and transferred to polyvinylidene difluoride membranes. Membrane blocking and incubation with antibodies were performed in Tris-buffered saline with 2% nonfat dry milk. Signals were revealed with chemiluminescence reagents and photographed by LAS-1000 mini (Fujifilm Corp, Tokyo, Japan). We also confirmed the loading protein dose by β-actin antibody staining as internal protein control. For analysis of filaggrin solubility and processing, epidermal lysates were prepared with RIPA buffer. Samples of precipitated proteins in the RIPA buffer were solubilized again in 8 mol/L urea before boiling in reducing SDS loading buffer.

Light Microscopy and Immunofluorescence Analysis

For light microscopy, we harvested the newborn pups' skin and the grafted skin, and fixed them for 24 hours in 10% neutral buffered formalin, dehydrated them in graded ethanol, and embedded them in paraffin. We cut 4-μm sections and stained them with H&E. For immunohistochemistry, the tissue samples were embedded in optimal cutting temperature compound (Sakura Finetechnical Corp., Tokyo, Japan). Frozen tissue sections were cut at a thickness of 5 μm. The sections were blocked with 1% bovine serum albumin (BSA) in PBS for 30 minutes at room temperature, and incubated in primary antibody solution in blocking buffer for 30 minutes at 37°C. Fluorescent labeling was performed with secondary antibodies, followed by propidium iodide (Sigma Chemical Co.) for 5 minutes at room temperature to counterstain nuclei. The stained samples were observed under an Olympus Fluoview confocal laser-scanning microscope (Olympus, Tokyo, Japan).

In Situ *Transglutaminase Activity*

The procedure for *in situ* transglutaminase 1 activity assay has been previously described.[7,8] In brief, unfixed cryosections of 5 μm were blocked with 100 mmol/L Tris-HCl pH7.4, 1% BSA for 30 minutes, and then incubated with 100 mmol/L Tri-HCl pH7.4, 5 mmol/L $CaCl_2$, 12 μmol/L monodansylcadaverine (Sigma) for 1 hour to detect transglutaminase 1 activity. For negative controls, EDTA was added to the monodansylcadaverine solution to a final concentration of 20 mmol/L. After stopping the transglutaminase 1 reaction with 10 mmol/L EDTA in PBS, sections were incubated with rabbit anti-dansyl antibody (Invitrogen Corp.) in 12% BSA/PBS for 3 hours. Sections were then incubated with fluorescein isothiocyanate-conjugated goat anti-rabbit antibody in 12% BSA/PBS for 30 minutes. Nuclei were counterstained by propidium iodide. The stained samples were observed under an Olympus Fluoview confocal laser-scanning microscope (Olympus).

Immunofluorescence Labeling of Cultured Cells

Immunofluorescence labeling of cultured cells was performed as previously described.[5] Briefly, primary/subcultured keratinocytes were fixed in 4% paraformaldehyde for 15 minutes and permeabilized with 0.1% Triton X-100 for 15 minutes at room temperature. Keratinocytes were blocked with 1% BSA in PBS for 30 minutes at room temperature,

and incubated in primary antibody solution in blocking buffer for 30 minutes at 37°C and fluorescence labeling was performed with secondary antibodies, followed by propidium iodide for 5 minutes at room temperature to counterstain nuclei. The stained samples were observed under an Olympus Fluoview confocal laser-scanning microscope (Olympus).

Electron Microscopy

Neonatal skin samples and skin grafts were fixed in 5% glutaraldehyde solution, post fixed in 1% OsO_4, dehydrated, and embedded in Epon 812 (TAAB Laboratories, Berkshire, UK). All of the samples were ultra-thin sectioned at a thickness of 70 nm, and stained with uranyl acetate and lead citrate. Photographs were taken using a Hitachi H-7100 transmission electron microscope (Hitachi, Tokyo, Japan).

Lipid Analysis

Lipid analysis was performed as previously reported.[9] Briefly, lipid analysis was done independently on three *Abca12*$^{-/-}$ neonates, two wild-type as controls, and two mature *Abca12*$^{-/-}$ skins 3 months after skin grafting and two mature wild-type skins 3 months after transplantation as control. We separated the epidermis from whole skin specimens of control and *Abca12*$^{-/-}$ mice by incubation in sterile water at 60°C for 1 minute and homogenized in 0.8 ml of PBS. A total lipid component was extracted from tissue homogenates of epidermis according to conventional methods.[9] Lipid analysis in epidermal lysates from neonates and grafted skin was performed by liquid chromatography, electrospray ionization mass spectrometry (LC-ESI-MS) using a HP 1100 liquid chromatography system (Agilent Technologies, Palo Alto, CA).

Measurement of Transepidermal Water Loss

Transepidermal water loss (TEWL) from the skin of neonatal mice and from skin grafted onto SCID mice was measured by evaporimeter (AS-VT100RS: Asahibiomed Corp., Yokohama, Japan), as described previously.[5] The AS-VT100RS utilizes the ventilated-chamber method for measuring TEWL. Its hygrometer measures the humidity of incoming air and of outgoing air that has passed over the test area of the skin, and TEWL is calculated from the difference. TEWL measurements were performed on the back of the neonates and the grafted skin onto the back of SCID mice.

Complementary DNA Microarray Analysis for the Gene Expression Profile

Total RNA isolated from primary/subcultured *Abca12*$^{-/-}$ keratinocytes was extracted as described above. Total RNA concentration was calculated spectrophotometrically, and quality control of RNA was analyzed with an Agilent 2100 Bioanalyzer (Agilent Technologies, Tokyo, Japan). mRNA/cDNA hybrids were generated via T7oligo dT primers, followed by addition of DNA polymerase and ligase (Filgen, Nagoya, Japan) to obtain double-stranded cDNA. The sample tagged with chemiluminescent substrate, Cy3 for the subcultured *Abca12*$^{-/-}$ keratinocytes, or Cy5 for the primary-cultured *Abca12*$^{-/-}$ keratinocytes, was hybridized on a microarray chip (Filgen Array mouse 32K, Filgen). We used a mixture of total RNAs from the two cultures for labeling reactions. Fluorescence images for Cy3 and Cy5 dye channels were obtained using a GenePix 4000B scanner (Axon Instruments, CA) and scan data images were analyzed using Microarray Data Analysis Tool version 3.0 software (Filgen).

Therapeutic Trial with Retinoids on Primary-Cultured Abca12$^{-/-}$ *Keratinocytes and Grafted Harlequin Ichthyosis Model Mice Skin*

To test the efficacy of a therapeutic trial on primary-cultured *Abca12*$^{-/-}$ keratinocytes, isotretinoin (purchased by Sigma Chemical Co., St. Louis, MO) was dissolved in dimethyl sulfoxide (DMSO). In addition, etretinate powder (a gift from Chugai Pharmaceuticals, Tokyo, Japan) was dissolved in sterile water.

Primary-cultured keratinocytes were grown in CnT-57 medium (Cellntec Advanced Cell Systems) and then switched into CnT-02 medium (Cellntec Advanced Cell Systems). Twenty-four hours later, the calcium concentration was changed to 1.2 mmol/L in CnT-02 medium with retinoids (10^{-6}mol/L isotretinoin or 10^{-6}mol/L etretinate) dissolved in DMSO or water. The final concentration of DMSO in medium was 0.01%. As control, keratinocytes were cultured in CnT-02 medium with 1.2 mmol/L calcium supplemented with 0.01% DMSO without retinoids. Forty-eight hours later, we extracted protein from keratinocytes.

In a therapeutic trial using grafted HI model mice skin, we dissolved several doses of isotretinoin in soy oil, and single doses (1, 10 mg/kg) of isotretinoin were administered orally into the grafted SCID mice 3 weeks after skin transplantation every day for 10 days.

Statistical Analysis

All statistical analyses were performed using student's *t*-tests with sample sizes indicated in the figure legends for each comparison that was made. *P* values of <0.05 were considered statistically significant.

Results

Abca12$^{-/-}$ *Neonatal Mouse Epidermis Exhibited Defective Lipid Distribution, Reduced Expression of Differentiation-Specific Proteins and Profilaggrin/Filaggrin Conversion Defects*

As we previously reported,[5] *Abca12*$^{-/-}$ mice (Figure 1B) were typically born with a smaller body size than that of wild-type mice (Figure 1A). Erythematous, rigid skin covered the entire body surface of *Abca12*$^{-/-}$ neonates.

Light microscopy showed a thick, compact cornified layers without the normal basket-weave appearance in the *Abca12*$^{-/-}$ neonatal skin (Figure 1D), compared with normal neonatal skin (Figure 1C). Electron microscopy of *Abca12*$^{-/-}$ neonatal skin showed numerous lipid droplets in the granular layer cell cytoplasm (Figure 1F). In wild-type neonatal skin, no lipid droplets were seen although normal keratohyalin granules were observed (Figure 1E). Immunofluorescence staining (Figure 1, G and H) showed Abca12 in wild-type but not abca12−/− mice, with the glucosylceramide/ceramide distribution remarkably sparse at the *Abca12*$^{-/-}$ neonatal mice granular/cornified layer interface (Figure 1J), compared with the intense labeling in the wild-type neonatal epidermis (Figure 1I). To verify these results in the neonatal *Abca12*$^{-/-}$ and wild-type skin, we performed lipid analysis using skin samples from both the *Abca12*$^{-/-}$ and wild-type neonates. Total amounts of epidermal ceramides were significantly reduced in *Abca12*$^{-/-}$ neonatal mice (Figure 1K). Particularly, amounts/compositions of the CER[EOS], ceramide classes consisting of ester-linked non-hydroxy fatty acids, ω-hydroxy fatty acids and 4-sphinnenines, in *Abca12*$^{-/-}$ neonatal epidermis were extremely small compared with control mice (see Supplemental Figure S1, A and B at *http://ajp.amjpathol.org*).

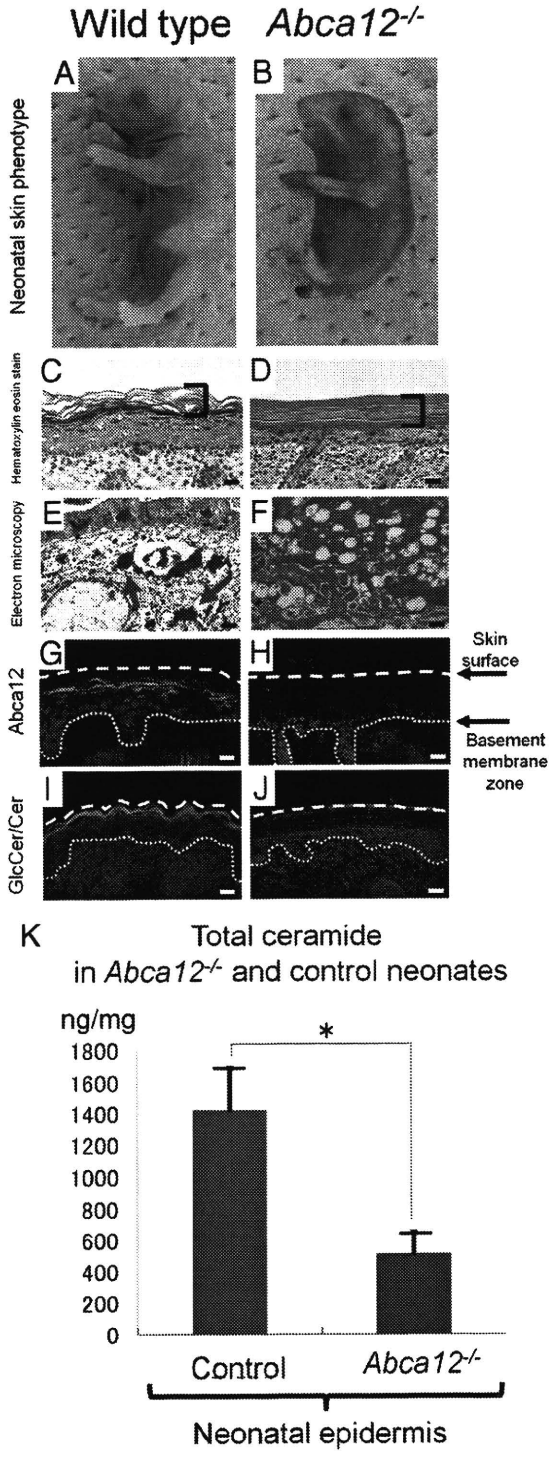

Immunofluorescence staining revealed that the keratinocyte differentiation (keratinization)-specific molecules, kallikrein 5 (KLK5), transglutaminase 1 (TGase1), and loricrin, were sparsely distributed in the upper epidermis of neonatal *Abca12*$^{-/-}$ mice (Figure 2A–J). Immunofluorescence staining for KLK5, a lamellar granule component, was weak in *Abca12*$^{-/-}$ neonatal mice granular layer (Figure 2B), in contrast to intense labeling in granular and lower cornified layers of wild-type neonatal skin (Figure 2A). *In situ* TGase1 activity assays with dansylcadaverine as a substrate showed neonatal *Abca12*$^{-/-}$ granular layer keratinocytes exhibited weak TGase1 activity restricted to the cytoplasm (Figure 2D), compared with distinct TGase1 activity with a more peripheral pattern throughout neonatal wild-type granular layer keratinocytes (Figure 2C). Immunofluorescence staining showed loricrin expressed sparsely within neonatal *Abca12*$^{-/-}$ granular layer cells (Figure 2F), compared with more intense expression in neonatal wild-type granular layer keratinocytes (Figure 2E).

KLK5, involucrin, TGase1, loricrin, and filaggrin mRNA expression was up-regulated in neonatal *Abca12*$^{-/-}$ epidermal keratinocytes (Figure 2K). In contrast, protein expression using epidermal extract, Western blotting demonstrated that loricrin and KLK5 protein expression was reduced in neonatal *Abca12*$^{-/-}$ epidermal keratinocytes compared with that in neonatal wild-type epidermis (Figure 2L). There were no significant differences in the pro-

Figure 1. *Abca12*$^{-/-}$ neonatal phenotype and lipid trafficking defects. **A** and **B:** Gross phenotypes of wild-type and *Abca12*−/− neonates. **C** and **D:** Light microscopy showed a thick compact cornified layer (bracket) without the normal basket-weave appearance in the *Abca12*$^{-/-}$ mouse skin (**D**), compared with normal neonatal skin (**C**) (H&E stain; original magnification, ×40) (Scale bars = 20 μm). **E** and **F:** An electron micrograph of the *Abca12*−/− neonatal skin showed numerous lipid droplets in the cytoplasm of the granular layer cells (**F, red arrows**). In the wild-type neonatal skin, no lipid droplets were seen and normal keratohyalin granules were observed (**E, red arrows**) (original magnification, ×3000) (Scale bars = 2 μm). **G** and **H:** By immunofluorescence staining, Abca12 expression (Alexa488, green) was detected in the wild-type neonatal mouse skin (**G**), but not in the *Abca12*$^{-/-}$ skin (**H**). **I** and **J:** Immunofluorescence staining showed the glucosylceramide/ceramide (GlcCer/Cer) (Alexa 488, green), a major lipid component of lamellar granules and an essential component of the epidermal permeability barrier, to be distributed remarkably sparse in the *Abca12*−/− neonatal mouse granular/cornified layer interface (**J**), compared with the intense labeling in the wild-type neonatal epidermis (**I**). **K:** In neonatal mice, total ceramides levels were significantly reduced in the epidermis of *Abca12*$^{-/-}$ mice. (*Abca12*−/− neonates, $n = 3$; control neonates, $n = 2$) (*$P < 0.01$). GlcCer, glucosylceramide; Cer, ceramide.

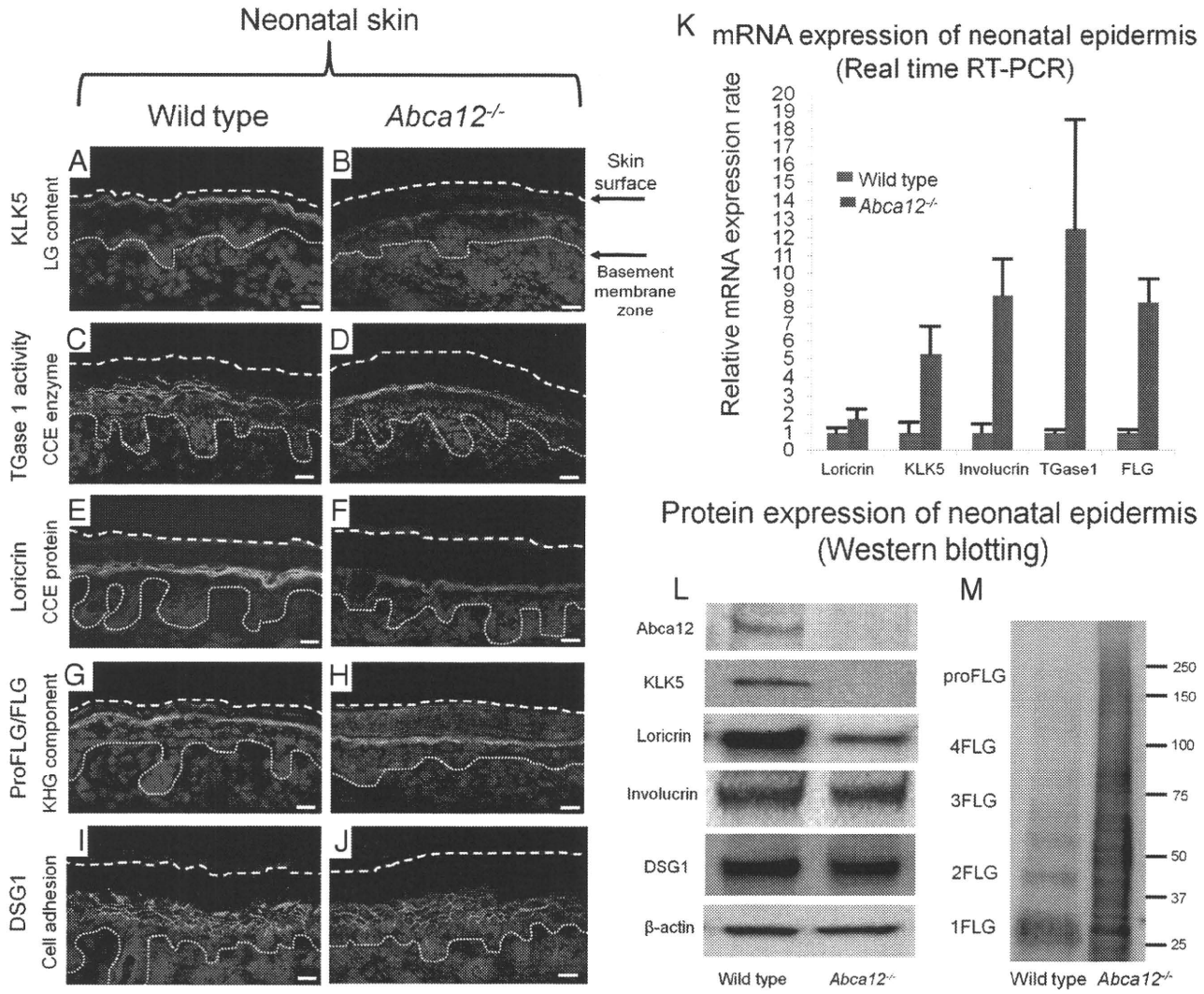

Figure 2. Reduced epidermal differentiation-associated molecules and defective conversion of profilaggrin to filaggrin in *Abca12*$^{-/-}$ neonates. **A** and **B:** Immunofluorescence staining for kallikrein 5 (KLK5) (Alexa488, green), one of the lamellar granule (LG) contents, was weak in the *Abca12−/−* neonatal mice granular keratinocyte layers (**B**), in contrast to its intense labeling in the granular layers and lower cornified layers of wild-type neonatal skin (**A**). **C** and **D:** *In situ* transglutaminase 1 (TGase1) activity assay (fluorescein isothiocyanate, green) with dansyl-cadaverine showed the granular layer keratinocytes in the *Abca12*$^{-/-}$ neonates had weak transglutaminase 1 activity only in the cytoplasm (**D**), compared with distinct transglutaminase 1 activity with the peripheral pattern throughout granular layer keratinocytes in the wild-type neonates (**C**). Cytoplasmic localization of transglutaminase 1 in *Abca12−/−* neonates indicated its inability to bind to the cell membrane and to therefore function at its proper place despite the significantly enhanced mRNA expression of transglutaminase 1 (see Figure 2K). **E** and **F:** Immunofluorescence staining showed loricrin (Alexa 488, green) expressed sparsely in the *Abca12*$^{-/-}$ neonatal mice granular layer (**F**), compared with its intense expression in the granular layer of the wild-type neonatal skin (**E**). **G** and **H:** Both *Abca12−/−* and wild-type neonatal skin showed intense profilaggrin/filaggrin (proFLG/FLG) (Alexa488, green) expression in the granular layer keratinocytes. However, in *Abca12*$^{-/-}$ neonatal skin, profilaggrin/filaggrin distribution was also observed throughout the cornified layers. **I** and **J:** Desmoglein 1(DSG1) (Alexa 488, green), a cell adhesion molecule unassociated with keratinization, was expressed at the cell periphery in the lower granular and spinous layers of the both *Abca12−/−* neonatal skin and wild-type mouse skin. (nuclear stain; propidium iodide, red, **dotted lines**, the skin surface). Original magnification ×40; Scale bars, 20 μm. **K:** mRNA expression of loricrin, kallikrein 5 (KLK5), involucrin, transglutaminase 1 (TGase1) and filaggrin (FLG) was up-regulated in the *Abca12*$^{-/-}$ neonatal epidermis. (*Abca12−/−* neonates, $n = 5$; wild-type neonates, $n = 5$, mRNA expression levels of wild-type neonatal epidermis = 1). **L:** Western blotting of epidermal extracts showed that protein expression of kallikrein 5 (KLK5) and loricrin was lower in the *Abca12*$^{-/-}$ neonatal epidermis (right) than in the wild-type neonatal epidermis (left). There were no significant differences of desmoglein 1(DSG1), involucrin, β-actin expressions between the *Abca12−/−* and wild-type epidermis. **M:** Western blotting with anti-profilaggrin/filaggrin antibody revealed the *Abca12*$^{-/-}$ neonatal epidermis (right) expressed more profilaggrin/filaggrin protein than wild-type neonatal epidermis (left). High molecular weight smear band corresponding to non-converted profilaggrin peptides were characteristic to the *Abca12−/−* neonatal epidermis. Western blotting using serial protein dilutions is shown in the supplemental Figure 2 (see Supplemental Figure S2 at *http://ajp.amjpathol.org*). KLK5, kallikrein 5; LG, lamellar granule; TGase1, transglutaminase 1; CCE, cornified cell envelope; FLG, filaggrin; KHG, keratohyalin granule; DSG1, desmoglein 1; proFLG, profilaggrin; 4FLG, filaggrin tetramer; 3FLG, filaggrin trimer; 2FLG, filaggrin dimer; 1FLG, filaggrin monomer.

tein expression of involucrin or control molecules unconnected with the keratinization process, β-actin, and desmoglein1 (DSG1), between *Abca12*$^{-/-}$ and wild-type neonatal epidermis.

Both *Abca12*$^{-/-}$ and wild-type neonatal skin demonstrated intense profilaggrin/filaggrin expression within granular layer keratinocytes (Figure 2, G and H). However, in *Abca12*$^{-/-}$ neonatal skin, profilaggrin/filaggrin distribution was also observed throughout all of the cornified layers (Figure 2H). Western blotting with anti-profilaggrin/filaggrin antibody revealed that neonatal *Abca12*$^{-/-}$ epidermis exhibited a greater amount of profilaggrin/filaggrin protein than that in the neonatal wild-type epidermis (Figure 2M). In particular, high molecular weight smear bands correspond-

ing to unconverted profilaggrin peptides were characteristic of neonatal *Abca12*$^{-/-}$ epidermis. Western blotting using the serial dilutions of protein showed that neonatal *Abca12*$^{-/-}$ epidermis exhibited a filaggrin monomer band, although the ratio of high molecular weight profilaggrin and its derivatives to filaggrin monomer in the *Abca12*$^{-/-}$ neonatal epidermis was extremely high compared with that of the wild-type neonatal epidermis (see Supplemental Figure S2A at *http://ajp.amjpathol.org*). The remaining high molecular bands in the neonatal *Abca12*$^{-/-}$ epidermis indicated defective profilaggrin conversion to filaggrin. Furthermore, we prepared 8 mol/L urea supernatants from precipitated proteins from the *Abca12*$^{-/-}$ neonatal epidermis in RIPA buffer. Western blotting with 8 mol/L urea supernatants confirmed that a proportion of filaggrin monomer, which is insoluble in the RIPA buffer exists in *Abca12*$^{-/-}$ neonatal epidermis (see Supplemental Figure S2B at *http://ajp.amjpathol.org*). In contrast, urea supernatants from precipitated proteins in RIPA buffer of wild-type neonatal epidermis showed only a faint band of filaggrin monomer. This finding indicated that majority of filaggrin monomer in the wild-type neonatal epidermis is soluble in RIPA buffer. These Western blotting results suggested that *Abca12*$^{-/-}$ neonatal epidermis exhibited not only defective profilaggrin/filaggrin conversion but also alteration of filaggrin monomer solubility. We also performed Western blotting with anti-loricrin antibody using 8 mol/L urea supernatant. Using 8 mol/L urea buffer as well as using RIPA buffer the loricrin band was faint in supernatant samples from the *Abca12*$^{-/-}$ neonatal epidermis (data not shown). Thus, the solubility of loricrin was unaltered in the *Abca12*$^{-/-}$ neonatal epidermis and we think that the alteration of solubility in the *Abca12*$^{-/-}$ neonatal epidermis is specific to filaggrin.

Improved Morphological Abnormalities, Corrected Lipid Distribution, and Restored Expression of Differentiation-Specific Molecules in Abca12$^{-/-}$ *Skin Grafts Maintained in Dry Environment*

Since *Abca12*$^{-/-}$ neonates die soon after birth, it was impossible to follow the phenotypic changes in the skin of *Abca12*$^{-/-}$ mice after birth. Therefore, we grafted their skin onto severe combined immunodeficient (SCID) mice and analyzed its morphological and biochemical alterations in the skin after birth/grafting.

Mature grafted *Abca12*$^{-/-}$ skin showed hairless keratotic plates at 3 weeks after transplantation onto the backs of SCID mice (Figure 3, A and B). Light microscopic observations revealed that hair follicles and shafts were buried in keratotic plugs in mature *Abca12*$^{-/-}$ skin (Figure 3, C and D). High power microscopy demonstrated that mature *Abca12−/−*skin showed discernible keratohyalin granules in the granular layers (Figure 3F) that were completely absent in *Abca12*$^{-/-}$ neonatal skin (Figure 1, E and F).

Immunofluorescence staining showed abca12 staining in wild-type but not abca12−/−mice and intense labeling of glucosylceramides/ceramides at the granular/cornified layer interface in mature grafted *Abca12*$^{-/-}$ skin (Figure 3, I and J), compared with a sparse distribution in the neonatal *Abca12−/−* mouse upper epidermis (Figure 1L). Electron microscopy of mature *Abca12*$^{-/-}$ skin showed many lipid droplets in the granular layer (Figure 3K), although the number of lipid droplets in the cornified layer was reduced when compared with that of neonatal skin (Figure 3L). Using lipid analysis, the amounts of both total ceramides and CER[EOS] were restored in mature *Abca12−/−* epidermis (Figure 3M, and see Supplemental Figure S1, C and D at *http://ajp.amjpathol.org*). These results indicate that mature grafted *Abca12*$^{-/-}$ epidermis was able to obtain a normal ceramide distribution together with a normal composition of ceramides.

Immunolabeling for differentiation-specific molecules confirmed improved keratinization during maturation of the grafted *Abca12*$^{-/-}$ skin (Figure 4, A–J). Intense KLK5 immunolabeling (Figure 4, A and B), *in situ* transglutaminase 1 (TGase1) activity (Figure 4, C and D), and loricrin immunostaining (Figure 4, E and F) were distributed throughout the granular layers in mature grafted *Abca12−/−* skin, compared with a sparse distribution in *Abca12*$^{-/-}$ neonatal skin (Figure 2, B, D, and F). Increased loricrin and KLK5 immunolabeling intensity was confirmed by Western blot analysis using epidermal extracts from mature grafted *Abca12−/−* epidermis (Figure 4K).

Mature grafted *Abca12*$^{-/-}$ skin showed intense profilaggrin/filaggrin labeling in the granular layer (Figure 4H), similar to the mature grafted wild-type skin (Figure 4G). The diffuse profilaggrin/filaggrin distribution throughout the cornified layers observed in *Abca12−/−* neonatal skin (Figure 2H) was not seen in mature grafted *Abca12*$^{-/-}$ skin (Figure 4H). Western blotting with anti-profilaggrin/filaggrin antibody revealed that the normal conversion of profilaggrin to filaggrin was restored in mature *Abca12−/−* epidermis (Figure 4K). Epidermal extracts of mature *Abca12*$^{-/-}$ skin at 3 weeks after transplantation showed low expression of high molecular weight smeared bands and, instead of those, exhibited intense filaggrin monomer bands, compared those with epidermal extracts of *Abca12−/−* neonatal skin.

Analysis of TEWL as a parameter of skin barrier defects, demonstrated *Abca12*$^{-/-}$ that neonatal back skin showed significantly greater TEWL than the wild-type neonatal skin ($n = 3$, $P < 0.001$) (Figure 4L). However, TEWL levels of mature *Abca12−/−* skin 3 weeks after the skin graft were significantly decreased as compared with levels of *Abca12*$^{-/-}$ neonatal skin ($n = 3$, $P < 0.001$).

Subcultured Abca12$^{-/-}$ *Mouse Keratinocytes Attained Normal Lipid Trafficking in the Cytoplasm, with Restoration of Differentiation-Specific Protein Expression and Intact Profilaggrin/ Filaggrin Conversion that Was Defective in Primary-Cultured* Abca12−/− *Mouse Keratinocytes*

To verify the results from grafted skin analysis, we performed a similar analysis using primary versus subcultured *Abca12*$^{-/-}$ keratinocytes. Immunolabeling with an-

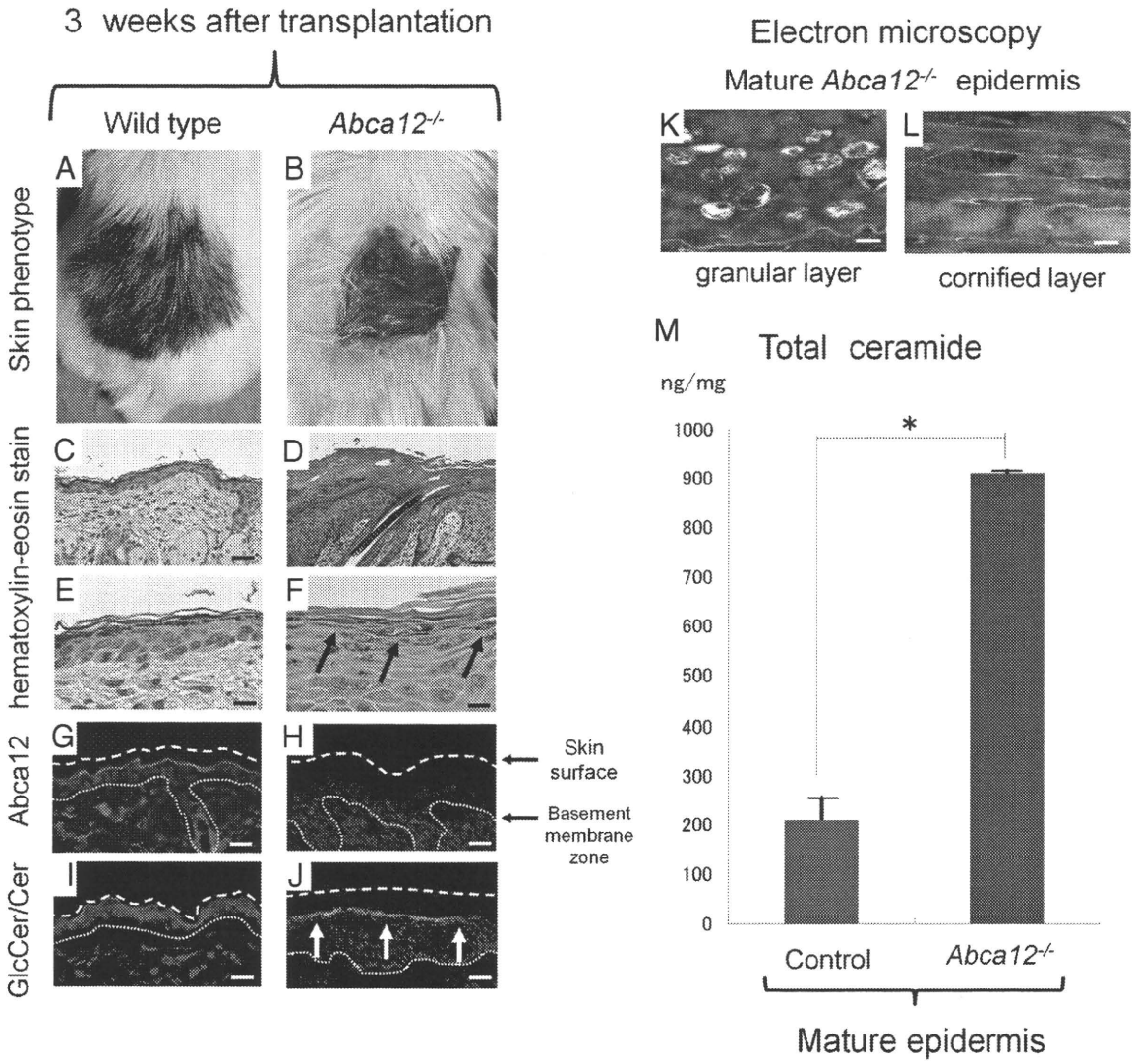

Figure 3. Altered morphology and improvement of ceramide deficiency during maturation of *Abca12*$^{-/-}$ skin. Gross (**A** and **B**) and microscopic (**C–L**) appearances of wild-type and *Abca12−/−* skin three weeks after transplantation onto SCID mice. **A:** Grafted skin of wild-type mice three weeks after transplantation. **B:** Grafted *Abca12*$^{-/-}$ skin three weeks after transplantation showed hairless keratotic plates. **C** and **D:** Light microscopic observation histology (H&E stain; original magnification ×40; Scale bars = 20 μm). Hair follicles and shafts were buried in keratotic plugs in the mature *Abca12−/−* skin three weeks after the skin graft (**D**). **E** and **F:** High power views (H&E stain; original magnification ×60; Scale bars = 10 μm). Mature *Abca12*$^{-/-}$ skin three weeks after transplantation showed discernible keratohyalin granule in the granular layers (**F**, **arrows**) that were lacked in *Abca12−/−* neonatal skin (see Figure 1, D and F). **G** and **H:** By immunofluorescence staining, Abca12 expression (Alexa488, green) was detected in the mature wild-type mouse skin (**G**), but not in the mature *Abca12*$^{-/-}$ skin (**H**). **I** and **J:** Immunofluorescence staining showed an intense distribution of glucosylceramide/ceramide (GlcCer/Cer) (Alexa 488, green) at the granular/cornified layer interface in mature *Abca12−/−* epidermis (**J**, **arrows**), compared with a sparse distribution in the neonatal *Abca12*$^{-/-}$ mouse upper epidermis (see Figure 1J). **K** and **L:** Ultrastructural observation of the grafted *Abca12−/−* skins three weeks after transplantation. There were many lipid droplets in the granular layer (**K**, **red arrowheads**), however the number of lipid droplets in the cornified layer (**L**, **red arrowheads**) was fewer than that of the neonatal *Abca12*$^{-/-}$ skin (see Figure 1F). Original magnification: ×10000 (**K**), ×5000 (**L**); Scale bars: 100 nm (**K**), 200 nm (**L**). **M:** From the lipid analysis of grafted skins, total ceramides levels of mature *Abca12*$^{-/-}$ epidermis were restored. (*Abca12−/−* grafted skins, $n = 2$; control grafted skins, $n = 2$) (*$P < 0.01$). GlcCer, glucosylceramide; Cer, ceramide

ti-glucosylceramide/ceramide antibody demonstrated a congested glucosylceramide/ceramide pattern in differentiated primary-cultured *Abca12−/−* mouse keratinocytes after first passage (Figure 5, B and E), compared with an uncongested, diffuse peripheral glucosylceramide/ceramide pattern in differentiated primary-cultured wild-type mouse keratinocytes (Figure 5, A and D). After 10 passages, subcultured *Abca12*$^{-/-}$ keratinocytes showed a widely distributed, diffuse glucosylceramide/ceramide staining pattern, similar to those of primary-cultured wild-type keratinocytes (Figure 5, C and F). Subcultured wild-type keratinocytes after 10 passages failed to show any alterations in lipid distribution (data not shown). These results indicate that lipid trafficking recovered during 10 passages of subculture in our *Abca12−/−* keratinocytes.

To investigate this altered differentiation state of primary/subcultured *Abca12*$^{-/-}$ keratinocytes, we performed real-time RT-PCR and immunoblot analysis (Figure 5, G and H). No significant differences were obtained in loricrin, KLK5, involucrin, TGase1 and filaggrin mRNA expression between primary-cultured *Abca12−/−* and wild-type keratinocytes (Figure 5G). Subcultured *Abca12*$^{-/-}$ keratinocytes showed higher loricrin, KLK5 and TGase1 mRNA

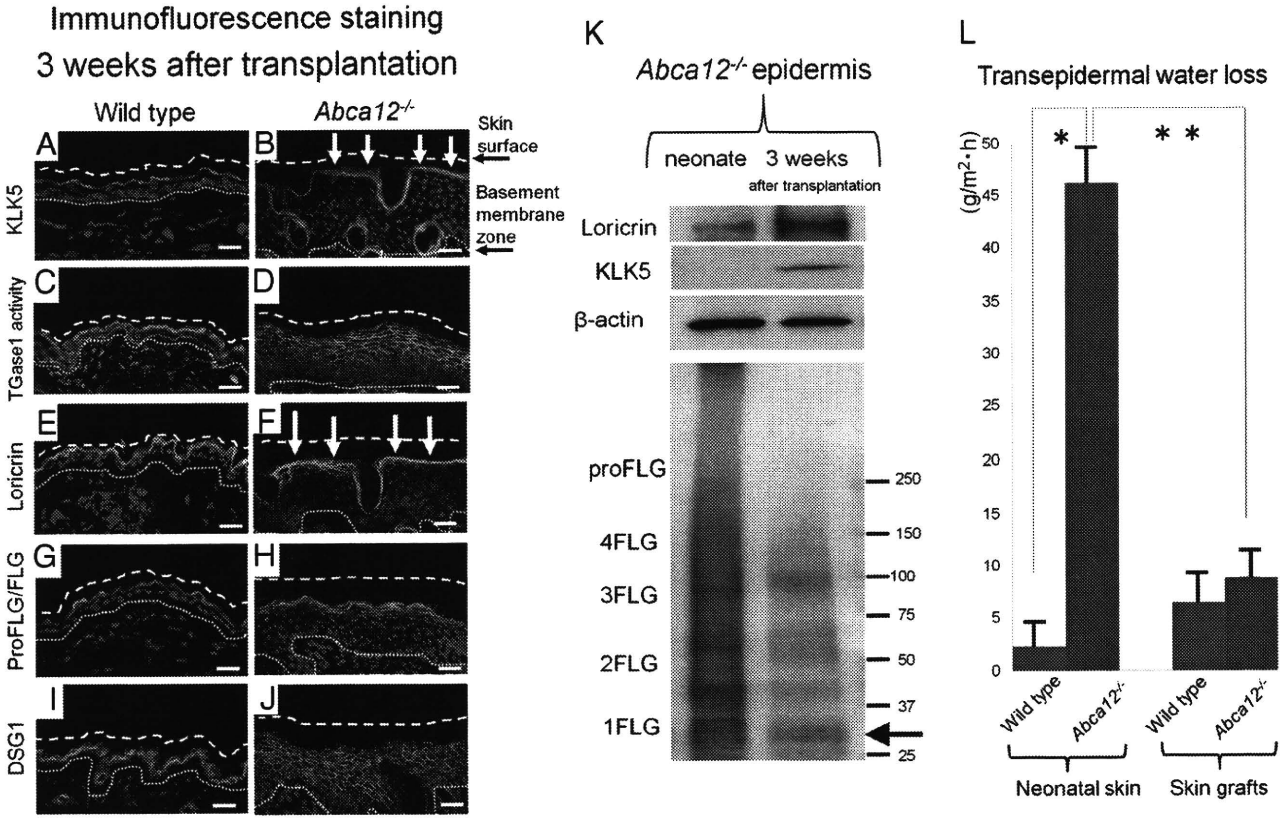

Figure 4. Improvement of previously disrupted differentiation-specific protein expression and defective skin barrier function in postnatal *Abca12*$^{-/-}$ skin. **A–J:** Immunolabeling for differentiation-specific molecules confirmed improved keratinization during maturation of the grafted *Abca12−/−* skin. Intense kallikrein 5 (KLK5) immunostaining (**A** and **B**, **white arrows**), *in situ* transglutaminase 1 (TGase1) activity labeling (**C** and **D**) and loricrin immunolabeling (**E** and **F**, **white arrows**) were seen throughout the granular layers in mature grafted *Abca12*$^{-/-}$ skin, compared with their sparse distribution in the *Abca12−/−* neonatal skin (see Figure 2, B, D and F). Increased loricrin and KLK5 immunolabeling intensity was confirmed by Western blot analysis using epidermal extracts from mature grafted *Abca12*$^{-/-}$ skin (**K**). Mature grafted *Abca12−/−* skin showed intense profilaggrin/filaggrin labeling in the granular layer (**H**), similar to the mature grafted wild-type skin (**G**). Diffuse profilaggrin/filaggrin staining in the entire cornified layers observed in *Abca12*$^{-/-}$ neonatal skin (see Figure 2H) disappeared in mature grafted *Abca12−/−* skin. Expression of desmoglein 1 (DSG1), unassociated with keratinization, was not altered in the grafted skin (**I** and **J**). Western blotting with anti-profilaggrin/filaggrin antibody revealed that normal conversion of profilaggrin to filaggrin was restored in mature *Abca12*$^{-/-}$ epidermis (**K**). Nuclear stain: propidium iodide, red; original magnification ×40; Scale bars = 20 μm. **L:** The barrier function in the transplanted skin was assessed by measuring transepidermal water loss (TEWL). The *Abca12−/−* neonates (red bar, left) showed significantly greater TEWL than the wild-type neonates (blue bar, left) showed ($^{*}P < 0.001$). TEWL levels of mature *Abca12*$^{-/-}$ epidermis three weeks after the skin graft (red bar, right) were significantly decreased as compared with levels of *Abca12−/−* neonatal skin (red bar, left) ($^{**}P < 0.001$), and was similar to levels of mature wild-type skin three weeks after the skin graft (blue bar, right). (*Abca12*$^{-/-}$ neonates, $n = 3$; wild-type neonates, $n = 3$; mature *Abca12−/−* skin, $n = 3$; mature wild-type skin, $n = 3$). KLK5, kallikrein 5; proFLG, profilaggrin; FLG, filaggrin; 4FLG, filaggrin tetramer; 3FLG, filaggrin trimer; 2FLG, filaggrin dimer; 1FLG, filaggrin monomer.

levels compared with primary-cultured *Abca12−/−* keratinocytes (Figure 5G). Blot extracts from differentiated primary-cultured *Abca12*$^{-/-}$ keratinocytes showed low expression of loricrin and KLK5 (Figure 5H), as observed in neonatal *Abca12−/−* mice epidermis (Figure 2L). However, extracts from subcultured *Abca12*$^{-/-}$ keratinocytes showed restoration of loricrin and KLK5 expression (Figure 5H), as observed in grafted mice epidermis (Figure 4K).

Western blotting with anti-profilaggrin/filaggrin antibody revealed that the filaggrin expression pattern had become normalized in subcultured *Abca12*$^{-/-}$ keratinocytes (Figure 5H). Cell lysates from10 passage-subcultured *Abca12−/−* keratinocytes showed an intense filaggrin monomer band that was faint in lysates from *Abca12*$^{-/-}$ primary first-passage keratinocytes.

Studies of subcultured *Abca12*$^{-/-}$ keratinocytes demonstrated restored differentiation, at least in part, similar to that observed in mature *Abca12−/−* skin grafts.

cDNA Microarray Analysis Revealed Up-Regulation of 22 Lipid Metabolic and/or Transport-Related Genes

To investigate the mechanism of restoration of intact keratinocytes differentiation in subcultured *Abca12*$^{-/-}$ keratinocytes, we analyzed whole gene expression profile of primary/subcultured *Abca12−/−* keratinocytes maintained under high Ca^{2+} condition using cDNA microarray methods. We obtained the 35,582 gene expression profile and observed 566 transcripts that were up-regulated more than three-fold in subcultured *Abca12−/−* keratinocytes compared with primary-cultured *Abca12*$^{-/-}$ keratinocytes. Among them, we searched for genes related to "lipid metabolism and/or lipid transporter function," and identified 22 specific transcripts including solute carrier family 22 member 7 (*Slc22a7*), prostaglandin D2 syn-

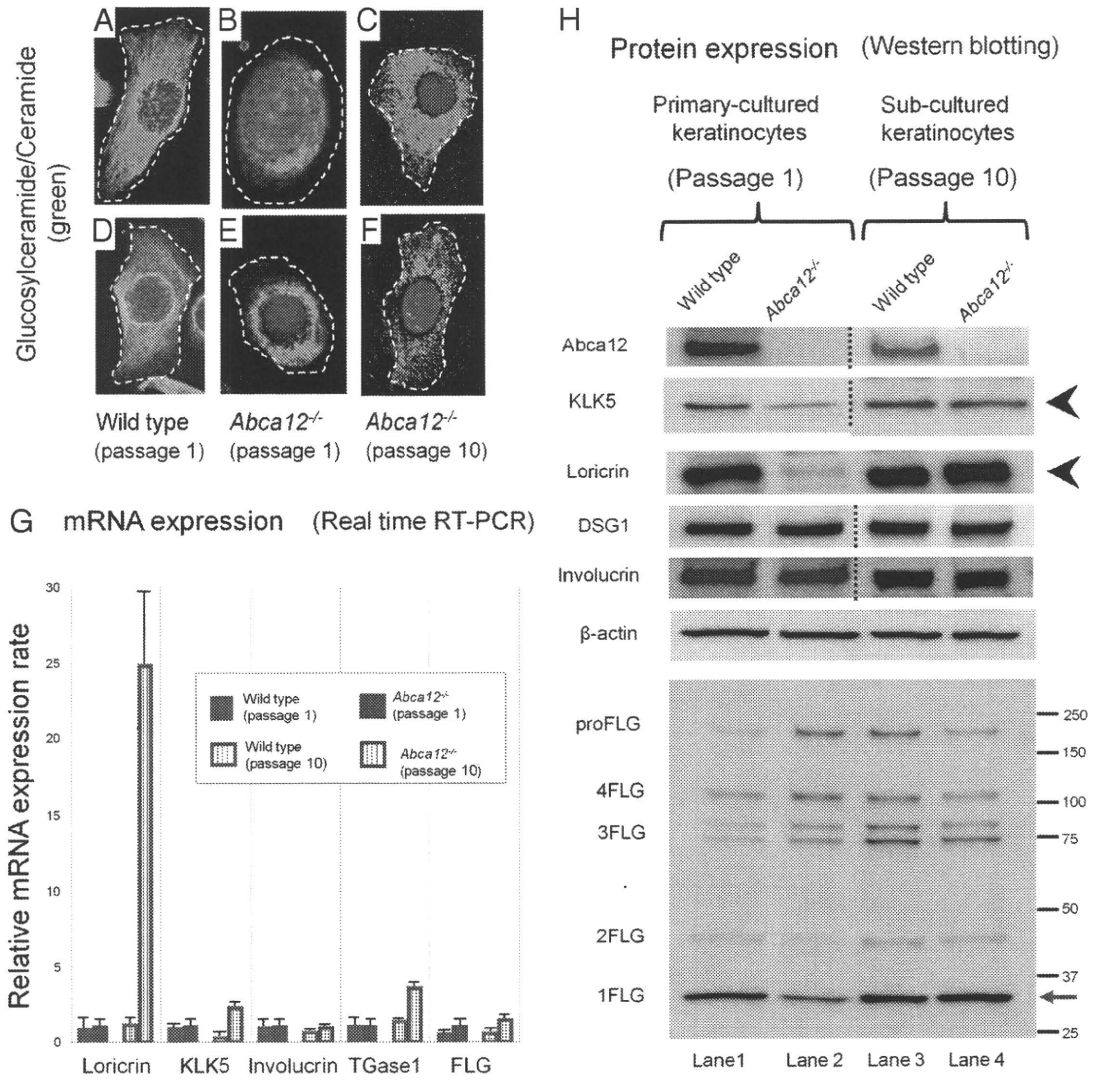

Figure 5. Subcultured *Abca12*$^{-/-}$ mouse keratinocytes exhibited restored intracytoplasmic localization of glucosylceramide/ceramide, protein expression of differentiation-specific molecules and profilaggrin conversion. **A–F:** Intracytoplasmic localization of glucosylceramide/ceramide in cultured keratinocytes. Immunolabeling demonstrated a congested pattern of glucosylceramide/ceramide (Alexa 488, green) in differentiated primary-cultured *Abca12−/−* mouse keratinocytes after first passage (**B** and **E**), in contrast with the uncongested, diffuse, peripheral pattern in the differentiated keratinocytes of a wild-type mouse (**A** and **D**). After 10 passages, subcultured *Abca12*$^{-/-}$ keratinocytes showed a widely distributed, diffuse glucosylceramide staining pattern (**C** and **F**), similar to those of wild-type keratinocytes. Subcultured wild-type keratinocytes after ten passages did not show any alterations in lipid distribution (data not shown). Nuclear stain: propidium iodide, red; original magnification ×60. **dotted lines** are the cell surface. **G:** There were no significant differences in loricrin, kallikrein 5 (KLK5), involucrin, transglutaminase 1 (TGase1), and filaggrin (FLG) mRNA expression between primary-cultured *Abca12−/−* keratinocytes (red bars, left) and primary-cultured wild-type keratinocytes (blue bars, left). Subcultured *Abca12*$^{-/-}$ keratinocytes (red bars, right) showed higher mRNA levels of loricrin, kallikrein 5, and transglutaminase 1 compared with primary-cultured *Abca12−/−* keratinocytes (red bars; left) and subcultured wild-type keratinocytes (blue bars, right). No significant difference was observed in involucrin and filaggrin mRNA expression. (primary-cultured *Abca12*$^{-/-}$, $n = 5$; primary-cultured wild-type, $n = 5$, subcultured *Abca12−/−* , $n = 5$; subcultured wild-type, $n = 5$, mRNA expression levels of *Abca12*$^{-/-}$ primary cultured keratinocytes = 1). **H:** Western blotting of differentiated cultured keratinocytes lysates under high Ca^{2+} condition showed that loricrin and KLK5 expression was lower in *Abca12−/−* primary-cultured keratinocytes (**lane 2**) than that of the wild-type primary-cultured keratinocytes (**lane 1**). Extracts from subcultured *Abca12*$^{-/-}$ keratinocytes showed restoration of loricrin and KLK5 expression (**lane 4**, **black arrowheads**). Western blotting with anti-profilaggrin/filaggrin antibody revealed that the *Abca12−/−* primary-cultured keratinocytes (**lane 2**) had reduced expression of mature filaggrin monomer than the wild-type primary-cultured keratinocytes (**lane 1**). In addition, the lysate from *Abca12*$^{-/-}$ primary-cultured keratinocytes exhibited plenty of high molecular weight bands, which indicated profilaggrin expression (**lane 2**). The filaggrin expression pattern was normalized in subcultured *Abca12−/−* keratinocytes (**lane 4**). Cell lysates from subcultured *Abca12*$^{-/-}$ keratinocytes showed an intense filaggrin monomer band that was faint in lysates from *Abca12−/−* primary first-passage keratinocytes (**lane 2** and **4**, **red arrow**). KLK5, kallikrein 5; TGase, transglutaminase; DSG1, desmoglein 1; proFLG, profilaggrin; 4FLG, filaggrin tetramer; 3FLG, filaggrin trimer; 2FLG, filaggrin dimer; 1FLG, filaggrin monomer.

thetase (*Ptgds*), annexin A9 (*Anxa9*), bactericidal/permeability-increasing protein-like 2 (*Bpil2*), phosphatidylethanolamine binding protein-2 variant 1 homolog (*Pbp2*), lipocalin 7 (*Tinagl*), *Gpr119*, solute carrier family 5 member 1 (*Slc5a1*), prostaglandin- endoperoxide synthase 2 (*Ptgs2*), and solute carrier family 30 member 1 (*Slc30a1*) (see Supplemental Table S1 at *http://ajp.amjpathol.org*). Notably, these genes included four ATP-binding transporter family members: *Abca17*, *Abca1a*, *Abcc5,* and *Abcb11* that were up-regulated at least three-fold.

Keratinocytes Treated with Retinoids Failed to Exhibit Normal Differentiation and Therapeutic Trials onto Grafted HI Model Mice Failed to Demonstrate Skin Phenotype Recovery

As treatment trials for primary keratinocytes, Western blotting revealed that primary-cultured wild-type keratinocytes expressed a large amount of loricrin peptide and had a decent amount of filaggrin monomer converted from profilaggrin (see Supplemental Figure S3 at *http://ajp.amjpathol.org*). Both isotretinoin (10^{-6} mol/L) and etretinate (10^{-6} mol/L) in the cultured medium for 48 hours lead to remarkable reduction of loricrin protein expression in primary-cultured wild-type keratinocytes, although filaggrin expression patterns were not altered. Neither isotretinoin (10^{-6} mol/L) nor etretinate (10^{-6} mol/L) improved the deficient loricrin protein expression or defective profilaggrin conversion in the primary-cultured *Abca12−/−* keratinocytes under high Ca^{2+} condition.

As a treatment trial for HI grafted skin, oral administration of various doses of isotretinoin (1 or 10 mg/kg daily for 10 consecutive days) to HI skin graft-recipient SCID mice demonstrated no change in the skin phenotype of grafted HI model mice skin at all (data not shown).

Discussion

Keratinocyte terminal differentiation (keratinization) is remarkably important to skin physiology and essential for epidermal function including barrier formation. Keratinization is a highly regulated process, involving a number of genes and pathways. Until now, abnormalities in keratinocyte differentiation have been reported in HI patients. Morphologically, Buxman et al[10] have reported that granular layers were absent or poorly formed in HI patient epidermis. Dale et al reported abnormal lamellar granules and defective profilaggrin conversion both in HI patients skin and their cultured keratinocytes.[11] Profilaggrin conversion to filaggrin is a key step during epidermal keratinization. Fleckman et al[12] reported that HI keratinocytes in 3 dimensional culture were unable to show the adequate differentiated epithelium and profilaggrin/filaggrin conversion. Recently, Thomas et al reported that the desquamation specific enzyme, kallikrein 5, and cathepsin D, were remarkably reduced in HI model skin using ABCA12 small interfering RNA knockdown keratinocytes.[13]

In the present study, we have demonstrated that keratinocyte differentiation was severely disrupted in both *Abca12*$^{-/-}$ HI neonatal model mouse skin and primary-cultured *Abca12−/−* keratinocytes. The present findings were consistent with previous reports of findings in HI patient's skin. Our neonatal HI model mice skin showed no apparent keratohyalin granules within any of their granular layer cells, which was consistent with Buxman's study.[10] Furthermore, our immunoblotting results confirmed defective profilaggrin/filaggrin conversion, which was consistent with the studies by Dale et al[11] and Fleckman et al.[12] Our immunostaining and immunoblotting results showed reduced expression of KLK5 in neonatal *Abca12*$^{-/-}$epidermis and primary-cultured *Abca12−/−* keratinocytes, which was consistent with the study by Thomas et al.[13] We therefore believe that our *Abca12*$^{-/-}$ HI model mouse faithfully reproduces the molecular condition thus far identified in human HI epidermis in addition to mimicking clinical phenotype.[5]

Zuo et al[6] suggested that loss of ABCA12 did not induce a block in the normal processing of profilaggrin to filaggrin in another reported ABCA12 deficient mouse strain, although the solubility of filaggrin was altered. We believe that our data are consistent with Zuo's study. In the present study, we showed high molecular weight bands in RIPA buffer extracted supernatant from neonatal *Abca12*$^{-/-}$epidermis. In study by Zuo et al,[6] similar high molecular weight bands were also seen by the Western blotting after detergent buffer supernatant extraction. We also showed an alteration in filaggrin monomer solubility using 8 mol/L urea supernatant, reproducing the findings of Zuo et al.[6] The major difference between these two studies is that Zuo et al[6] showed no filaggrin monomer band after detergent buffer supernatant extraction in their ABCA12 deficient mouse skin. In contrast, we detected filaggrin monomer band in RIPA supernatant of our *Abca12−/−*neonatal epidermis. This finding might result from differences in lysis buffer, tissue sample

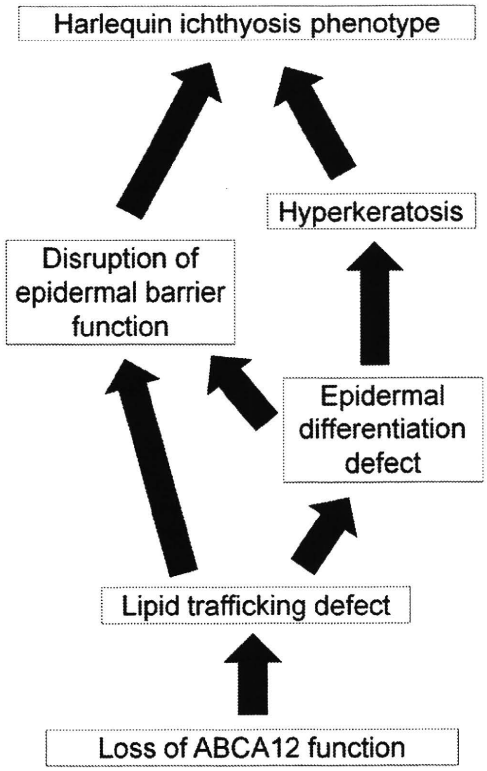

Figure 6. Putative pathomechanism of harlequin ichthyosis. Based on our results, we propose a novel pathogenetic mechanism underlying harlequin ichthyosis (HI). Our results suggested that a lipid trafficking defect due to loss of ABCA12 function leads to not only malformation of the epidermal lipid barrier but also "an epidermal differentiation defect." In our hypothesis, the severe hyperkeratosis, a characteristic phenotype of HI skin, is not a hyperkeratosis compensating for any barrier insufficiency, but a hyperkeratosis due to both defective differentiation and an abnormal desquamation process. The present scenario explains both the HI skin phenotype at/after birth and even *in utero*.

(whole skin or only epidermis), or harvest time (E18.5 or neonate). We conclude that neonatal *Abca12*$^{-/-}$ epidermis exhibits not only defective profilaggrin/filaggrin conversion but also alterations in filaggrin monomer solubility, as previously suggested by Dale et al,[11] Fleckman et al,[12] and Zuo et al.[6]

Based on our results, we propose several new pathogenetic mechanisms for HI (Figure 6). Our results suggest that "an epidermal differentiation defect" is the major pathomechanism in HI. This new pathogenesis model is furthermore able to resolve the conflicting "the barrier insufficiency" theory with the (human) HI clinical phenotype. Our novel "epidermal differentiation" theory can explain HI skin phenotype at birth and even *in utero*. In our theory, severe hyperkeratosis, characteristic of the HI skin phenotype, was not a compensative hyperkeratosis for barrier insufficiency, but a hyperkeratosis due to defective differentiation and desquamation processes.

Epidermal differentiation defects in our HI model mice suggest that ABCA12 lipid trafficking, which occurs during the early stages of keratinization, is a crucial step for correct keratinocyte terminal differentiation. In normal granular layer keratinocytes, ABCA12 transports lipids and forms lamellar granules.[3] Just after the extrusion of lipids from lamellar granules at the granular/cornified layer interface, loricrin accumulates at the cell periphery and is integrated into the insoluble cornified cell envelope by transglutaminases.[14] At the final phase of terminal differentiation, profilaggrin undergoes many post-translational modifications, including conversion to functional filaggrin monomers, which aid in the bundling of keratin intermediate filaments and formation of the cornified cell envelope.[14–16] Serine proteases including KLK5 are involved in the desquamation process after keratinization.[17] Our present results suggest that defective lipid trafficking and lamellar granule formation fail to initiate the normal sequence of events of the keratinization process. These facts indicate that ABCA12 lipid trafficking is essential to precisely regulate keratinocyte differentiation.

Interestingly, mature grafted HI model mouse skin and subcultured *Abca12*$^{-/-}$ keratinocytes showed improvement in the *Abca12−/−*-related abnormalities observed in neonatal skin and primary-cultured keratinocytes, such as the aberrant ceramide distribution, reduced differentiation-specific protein expression and profilaggrin/filaggrin conversion defects. Similar to our *Abca12*$^{-/-}$ model mouse skin, improvement in skin manifestations during maturation was observed in several other ichthyotic model mice. Loricrin knockout mice exhibit shiny translucent skin at birth although these mice showed a normal skin phenotype at 4 to 5 days after birth.[18] Biochemically, the mice showed increased protein expression of small proline rich proteins, which are also cornified cell envelope components during skin maturation.[18] Mature 12R-lipoxygenase knockout mouse skin showed recovery of skin barrier function and restoration of profilaggrin conversion after maturation, which had been lacking in the neonatal mice.[19,20] In addition, mature transglutaminase 1 knockout mouse skin also showed skin barrier functional recovery, although exact compensation mechanisms other than hyperkeratosis were not identified.[21]

To find any clues for the mechanism of compensation in *Abca12*$^{-/-}$ mice, we conducted cDNA microarray analysis. We could find that several transporters including four ATP-binding cassette (ABC) transporter family genes were up-regulated in subculture compared with primary-cultured *Abca12−/−* keratinocytes. We consider these up-regulated ABC transporters as prime candidate genes to compensate for the loss of ABCA12 function. These lipid transport/metabolism-related molecules might help in lipid trafficking and/or recovery of epidermal differentiation in *Abca12*$^{-/-}$ keratinocytes.

The recovery of skin barrier function and self-improvement of epidermal differentiation defects in mature *Abca12*$^{-/-}$ skin gave us important clues to aid in treatment of HI patients. Infants affected with HI frequently die within the neonatal period, although the survival rate of HI newborns has increased recently with the arrival of neonatal intensive care regimes with retinoid administration.[22–26] Our observations in mature *Abca12−/−* skin further confirmed that the early neonatal period is a critical time defining the prognosis. In this context, neonatal intensive care for HI newborns in the initial neonatal period is important for their survival.

We had already tried systemic retinoid administration to pregnant mice as a fetal therapy, although neither improvement of the skin manifestations nor extension of the survival period was obtained in the *Abca12*$^{-/-}$ newborns from the treated-mother mice.[5] Based on the clinical efficacy of retinoids to HI patients,[22–26] we conducted retinoid administration to the primary-cultured *Abca12−/−* keratinocytes. We could not detect any recovery of differentiation defects in the primary-cultured *Abca12*$^{-/-}$ keratinocytes treated with retinoids. These results of our therapeutic trials to fetuses in the previous report[5] and to primary keratinocytes in this study indicated that retinoids may be ineffective for modifying the epidermal differentiation defects during the fetal period. These facts were consistent with the known effects of retinoids, which enhance proliferation and suppress differentiation of keratinocytes.[27,28] Further, we performed a treatment trial on grafted SCID mice using systemic isotretinoin administration. Oral administration of any dose of isotretinoin (either 1 or 10 mg/kg daily, for 10 consecutive days) to the HI-skin-grafted SCID mice failed to improve the skin phenotype of grafted HI skin at all. We failed to obtain any clue to understand the reason why retinoids are only effective for HI patients from our present study.

In conclusion, we have demonstrated that disrupted epidermal keratinocyte differentiation is the pathomechanism involved in HI, and that during maturation, *Abca12*$^{-/-}$ epidermal keratinocytes regain normal keratinocyte differentiation. This restoration of differentiation is likely to be associated with the skin phenotype improvement observed in HI survivors.

Acknowledgment

We thank Dr. James R. McMillan for proofreading this manuscript.

References

1. Akiyama M: Pathomechanisms of harlequin ichthyosis and ABCA transporters in human diseases. Arch Dermatol 2006, 142:914–918
2. Hovnanian A: Harlequin ichthyosis unmasked: a defect of lipid transport. J Clin Invest 2005, 115:1708–1710
3. Akiyama M, Sugiyama-Nakagiri Y, Sakai K, McMillan JR, Goto M, Arita K, Tsuji-Abe Y, Tabata N, Matsuoka K, Sasaki R, Sawamura D, Shimizu H: Mutations in lipid transporter ABCA12 in harlequin ichthyosis and functional recovery by corrective gene transfer. J Clin Invest 2005, 115:1777–1784
4. Kelsell DP, Norgett EE, Unsworth H, Teh MT, Cullup T, Mein CA, Dopping-Hepenstal PJ, Dale BA, Tadini G, Fleckman P, Stephens KG, Sybert VP, Mallory SB, North BV, Witt DR, Sprecher E, Taylor AE, Ilchyshyn A, Kennedy CT, Goodyear H, Moss C, Paige D, Harper JI, Young BD, Leigh IM, Eady RA, O'Toole EA: Mutations in ABCA12 underlie the severe congenital skin disease harlequin ichthyosis. Am J Hum Genet 2005, 76:794–803
5. Yanagi T, Akiyama M, Nishihara H, Sakai K, Nishie W, Tanaka S, Shimizu H: Harlequin ichthyosis model mouse reveals alveolar collapse and severe fetal skin barrier defects. Hum Mol Genet 2008, 17:3075–3083
6. Zuo Y, Zhuang DZ, Han R, Isaac G, Tobin JJ, McKee M, Welti R, Brissette JL, Fitzgerald ML, Freeman MW: ABCA12 maintains the epidermal lipid permeability barrier by facilitating formation of ceramide linoleic esters. J Biol Chem 2008, 283:36624–36635
7. Akiyama M, Smith LT, Shimizu H: Expression of transglutaminase activity in developing human epidermis. Br J Dermatol 2000, 142:223–225
8. Raghunath M, Hennies HC, Velten F, Wiebe V, Steinert PM, Reis A, Traupe H: A novel in situ method for the detection of deficient transglutaminase activity in the skin. Arch Dermatol Res 1998, 290: 621–627
9. Masukawa Y, Narita H, Shimizu E, Kondo N, Sugai Y, Oba T, Homma R, Ishikawa J, Takagi Y, Kitahara T, Takema Y, Kita K: Characterization of overall ceramide species in human stratum corneum. J Lipid Res 2008, 49:1466–1476
10. Buxman MM, Goodkin PE, Fahrenbach WH, Dimond RL: Harlequin ichthyosis with epidermal lipid abnormality. Arch Dermatol 1979, 115:189–193
11. Dale BA, Holbrook KA, Fleckman P, Kimball JR, Brumbaugh S, Sybert VP: Heterogeneity in harlequin ichthyosis, an inborn error of epidermal keratinization: variable morphology and structural protein expression and a defect in lamellar granules. J Invest Dermatol 1990, 94:6–18
12. Fleckman P, Hager B, Dale BA: Harlequin ichthyosis keratinocytes in lifted culture differentiate poorly by morphologic and biochemical criteria. J Invest Dermatol 1997, 109:36–38
13. Thomas AC, Tattersall D, Norgett EE, O'Toole EA, Kelsell DP: Premature terminal differentiation and a reduction in specific proteases associated with loss of ABCA12 in Harlequin ichthyosis. Am J Pathol 2009, 174:970–978
14. Bickenbach JR, Greer JM, Bundman DS, Rothnagel JA, Roop DR: Loricrin expression is coordinated with other epidermal proteins and the appearance of lipid lamellar granules in development. J Invest Dermatol 1995, 104:405–410
15. Candi E, Schmidt R, Melino G: The cornified envelope: a model of cell death in the skin. Nat Rev Mol Cell Biol 2005, 6:328–340
16. Denecker G, Ovaere P, Vandenabeele P, Declercq W: Caspase-14 reveals its secrets. J Cell Biol 2008, 180:451–458
17. Meyer-Hoffert U, Wu Z, Schroder JM: Identification of lympho-epithelial Kazal-type inhibitor 2 in human skin as a kallikrein-related peptidase 5-specific protease inhibitor. PLoS One 2009, 4:e4372
18. Koch PJ, de Viragh PA, Scharer E, Bundman D, Longley MA, Bickenbach J, Kawachi Y, Suga Y, Zhou Z, Huber M, Hohl D, Kartasova T, Jarnik M, Steven AC, Roop DR: Lessons from loricrin-deficient mice: compensatory mechanisms maintaining skin barrier function in the absence of a major cornified envelope protein. J Cell Biol 2000, 151:389–400
19. Epp N, Furstenberger G, Muller K, de Juanes S, Leitges M, Hausser I, Thieme F, Liebisch G, Schmitz G, Krieg P: 12R-lipoxygenase deficiency disrupts epidermal barrier function. J Cell Biol 2007, 177: 173–182
20. de Juanes S, Epp N, Latzko S, Neumann M, Furstenberger G, Hausser I, Stark HJ, Krieg P: Development of an Ichthyosiform Phenotype in Alox12b-Deficient Mouse Skin Transplants. J Invest Dermatol 2009, 129:1429–1436
21. Kuramoto N, Takizawa T, Takizawa T, Matsuki M, Morioka H, Robinson JM, Yamanishi K: Development of ichthyosiform skin compensates for defective permeability barrier function in mice lacking transglutaminase 1. J Clin Invest 2002, 109:243–250
22. Prasad RS, Pejaver RK, Hassan A, Dusari S, Wooldridge MA: Management and follow-up of harlequin siblings. Br J Dermatol 1994, 130:650–653
23. Lawlor F, Peiris S: Harlequin fetus successfully treated with etretinate. Br J Dermatol 1985, 112:585–590
24. Ward PS, Jones RD: Successful treatment of a harlequin fetus. Arch Dis Child 1989, 64:1309–1311
25. Haftek M, Cambazard F, Dhouailly D, Reano A, Simon M, Lachaux A, Serre G, Claudy A, Schmitt D: A longitudinal study of a harlequin infant presenting clinically as non-bullous congenital ichthyosiform erythroderma. Br J Dermatol 1996, 135:448–453
26. Singh S, Bhura M, Maheshwari A, Kumar A, Singh CP, Pandey SS: Successful treatment of harlequin ichthyosis with acitretin. Int J Dermatol 2001, 40:472–473
27. Eichner R, Kahn M, Capetola RJ, Gendimenico GJ, Mezick JA: Effects of topical retinoids on cytoskeletal proteins: implications for retinoid effects on epidermal differentiation. J Invest Dermatol 1992, 98:154–161
28. Eichner R: Epidermal effects of retinoids: in vitro studies. J Am Acad Dermatol 1986, 15:789–797

Neutral Lipid Storage Leads to Acylceramide Deficiency, Likely Contributing to the Pathogenesis of Dorfman–Chanarin Syndrome

Journal of Investigative Dermatology (2010) **130,** 2497–2499; doi:10.1038/jid.2010.145; published online 3 June 2010

TO THE EDITOR

Dorfman–Chanarin syndrome (DCS) is an autosomal recessive, neutral lipid storage disorder with ichthyosis (NLSDI) due to loss-of-function mutations in *CGI-58* (a/β-hydrolase domain-containing protein 5, *ABHD5*). *CGI-58* encodes a 39 kDa protein, a widely expressed cofactor in mammalian tissues including epidermis that activates adipose triglyceride (TG) lipase (reviewed in Schweiger *et al.*, 2009; Yamaguchi and Osumi, 2009), as well as other still unidentified TG lipases (Radner *et al.*, 2009). CGI-58 expression increases during keratinocyte differentiation; and conversely, knockdown of this cofactor reduces keratinocyte differentiation (Akiyama *et al.*, 2008). Epidermal permeability barrier defects due in part to lamellar/nonlamellar phase separation of secreted lipids, within extracellular domains of the stratum corneum (SC) have been proposed to account for the barrier abnormalities in NLSDI (Elias and Williams, 1985; Demerjian *et al.*, 2006). Although defective extracellular lipid organization clearly is one contributor (Demerjian *et al.*, 2006), we assessed whether diversion of free fatty acid (FA) into esterified lipids causes lipid abnormalities that further impact barrier formation.

We recently reported a DCS patient with a, to our knowledge, previously unreported *CGI-58* missense mutation (Ujihara *et al.*, 2010), exhibiting abnormal barrier-related structures resembling other NLSDI patients (Demerjian *et al.*, 2006). Both mild and severely affected ichthyotic SCs revealed increased TG and decreased FA levels in comparison with SC fraction from normal subjects (Ujihara *et al.*, 2010). Pertinently, the extent of the increase in TG levels correlated with site-specific differences in the severity of the dermatosis (Ujihara *et al.*, 2010). These observations suggest that divergence of FA to TG contributes to disease phenotype in NLSDI.

We previously showed that ω-*O*-acylceramides (or acylCer) that have only been identified in differentiated layers of epidermis in terrestrial mammals are essential constituents of the epidermal permeability barrier; that is, lack of acylCer formation results in neonatal death due to abnormal epidermal permeability barrier function (Vasireddy *et al.*, 2007). AcylCer and the de-ω-*O*-esterified form (ω-hydroxy [ω-OH] ceramide [Cer]) are present either as free (unbound) or bound species (Uchida and Holleran, 2008). The latter form a continuous lipid monolayer, the corneocyte-bound lipid envelope (CLE); that is, a pool of ω-OH Cer, which is covalently bound to the external surface of the cornified envelope (Uchida and Holleran, 2008). Although free acylCer are critical for the formation of the lamellar membranes (Bouwstra *et al.*, 1998), our previous studies suggest the CLE is also important for normal permeability barrier function (Behne *et al.*, 2000). Prior studies suggest that FAs derived from TG are used in the ω-*O*-esterification step to form acylCer (Wertz and Downing, 1990). Moreover, TG, linoleate, and acylCer, but not phosphoglycerolipid content, decline in acyl-CoA: diacylglycerol acyltransferase-2-deficient mice, which also show a permeability barrier abnormality (Stone *et al.*, 2004). In addition, linoleate, which is the predominant FA that is used for ω-*O*-esterification, is enriched in TG in mouse skin (Stone *et al.*, 2004). Thus, we hypothesized that a failure of TG hydrolysis, due to abnormal CGI-58 function, could attenuate permeability barrier formation in NLSDI by decreasing acylCer content of affected SC.

Therefore, we first investigated the lipid profiles in solvent extracts of SC from this DCS patient (Ujihara *et al.*, 2010). Neither cholesterol (Ujihara *et al.*, 2010) nor total (bulk) Cer (Figure 1a) content was altered. Yet, Cer comprises a family of at least 10 species in humans (Uchida and Holleran, 2008). Because not only bulk Cer amount but also each individual Cer species contributes to the formation of competent lamellar structures required for barrier function (Bouwstra *et al.*, 1998), we subfractionated Cer into individual Cer species. Whereas the major Cer subfractions, NS (Cer 2), NP (Cer 3), and AS (Cer 5) were not significantly altered, acylCer were present at only trace levels in the patient sample (Figure 1b; because sample amounts were limited, other minor Cer species; that is, EOH (Cer 4), AP (Cer 6) (AP), AH (Cer 7) could not be quantitated) (abbreviations for Cer structures are according to Motta. *et al.* and Robson K. *et al.*, details reviewed in Uchida and Holleran, 2008).

Abbreviations: acylCer, acylceramide; Cer, ceramide; CGI-58, Comparative Gene Identification-58; CLE, bound lipid envelope; DCS, Dorfman–Chanarin syndrome; FA, fatty acid; KC, keratinocyte; NLSDI, neutral lipid storage disorder with ichthyosis; ω-OH, omega hydroxy; SC, stratum corneum; TG, triacylglyceride

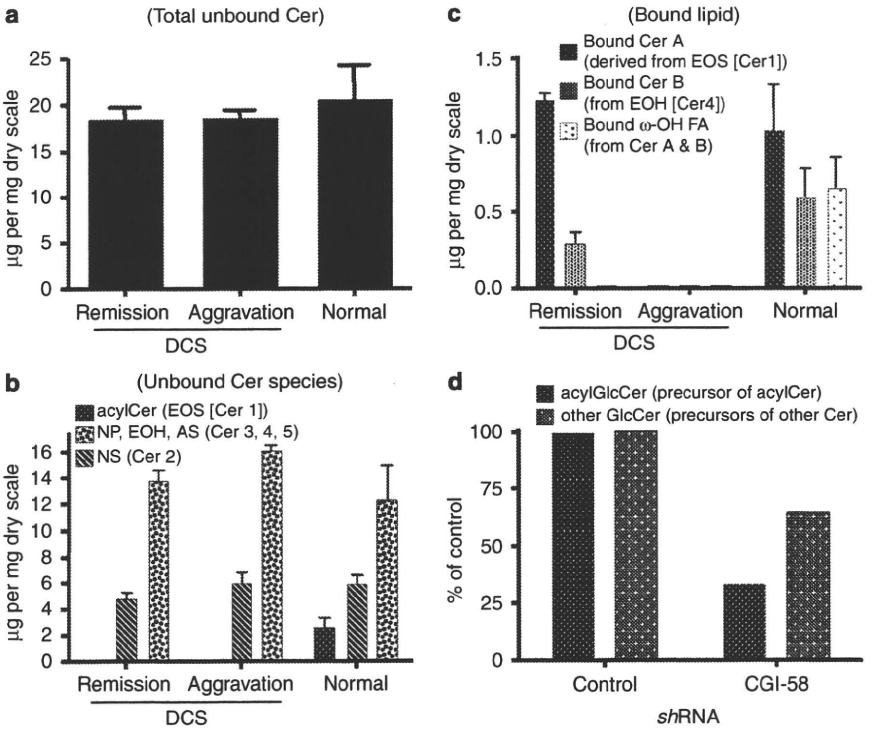

Figure 1. Lipid profile in the stratum corneum. Both unbound acylCer and bound ω-OH Cer deficiencies occur in a Dorfman–Chanarin syndrome (DCS) stratum corneum (SC) (**a–c**), whereas diminished CGI-58 expression decreases acylglucosylCer production (**d**). Normal SC from sunburn lesion as controls. CHK transfected with lentivirus-expressed shRNA (CGI-58 or control vector) were cultured in differentiation-inducing medium (Uchida *et al.*, 2001). Lipids were isolated from SC or cells and quantitated using thin-layer chromatography-scanning densitometry as described previously (Uchida *et al.*, 2001). $n=1$ (DC) and $n=3$ (normal). All studies were approved by the institutional ethics review boards (Kochi University and University of California, San Francisco) and were performed according to the Declaration of Helsinki Principles.

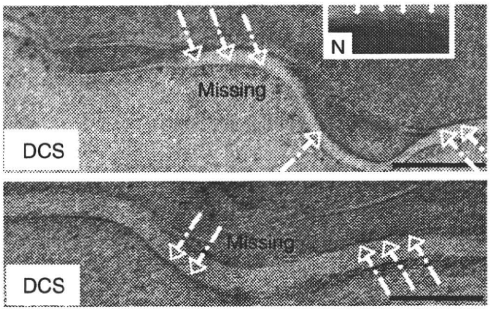

Figure 2. Electron micrographs display lack of continuous lipid monolayer, CLE, in the SC from two DCS patients (Demerjian *et al.*, 2006) vs. normal subject (inset, N). Skin samples were fixed in Karnovsky's fixative, and post-fixed with ruthenium tetroxide or osmium tetroxide, as previously described (Behne *et al.*, 2000). Ultrathin sections were examined, after further contrasted with lead citrate, with a Zeiss 10A (Carl Zeiss, Thornwood, NY) (Behne *et al.*, 2000). Arrows (with solid line, presence and with dotted line, absence) indicate CLE structures. Bars = 100 nm.

Not only bound ω-OH Cer, but also bound ω-OH FA (resulting from the subsequent hydrolysis of some bound ω-OH Cer by ceramidase) decline significantly in DCS (Figure 1c). As with TG accumulation (Ujihara *et al.*, 2010), the decrease in these bound lipids reflects disease severity. Accordingly, this patient, as well as in two additional DCS patients (Demerjian *et al.*, 2006), lacked CLE on ultrastructural analysis of affected SC (Figure 2).

Finally, we investigated whether the decreased acylCer in DCS is due to a gain-of-function of mutation in *CGI-58*, rather than a deficiency of TG-derived FA. A substantial decrease in acylglucosylCer (= acylCer precursor), but not in other glucosylCer species, was evident in lentivirus-expressed CGI-58 shRNA-treated cultured human keratinocytes (Figure 1d). Hence, by facilitating the lipolysis of TG, CGI-58 provides FA for ω-*O*-esterification leading to acylCer formation. The recent demonstration of a lethal, postnatal permeability barrier defect and deficiency of both acylCer and bound ω-OH Cer in *cgi-58*-null mice (Radner *et al.*, 2009) further supports this conclusion.

We conclude from these and previous studies that CGI-58 not only facilitates TG lipolysis but also provides FA for the ω-*O*-esterification of Cer leading to acylCer production, as well as bound ω-OH Cer generation leading to CLE formation (see Supplementary Figure S1 online). These studies highlight that the deficiency of an essential barrier constitute, acylCer, likely contributes to the permeability barrier

abnormality in DCS. Although the function of the CLE is still unclear, a role as a necessary scaffold for the lamellar bilayer organization is likely (Uchida and Holleran, 2008). Thus, CLE deficiency, coupled with disorganization of extracellular lamellar bilayers, likely merge to provoke the barrier abnormality in NLSDI (see Supplementary Figure S2 online). Finally, to overcome this metabolic disadvantage in forming the epidermal permeability barrier, epidermal proliferation likely increases, which in turn results in hyperkeratosis, phenotypic features common to virtually all of the ichthyoses (Demerjian *et al.*, 2006; Akiyama *et al.*, 2008), that is, 'A compromised permeability barrier 'drives' the hyperproliferative epidermis in NLSDI and other ichthyoses' (Elias *et al.*, 2008).

CONFLICT OF INTEREST
The authors state no conflict of interest.

ACKNOWLEDGMENTS
We acknowledge Ms Sally Pennypacker for technical support with the cell cultures. This study was supported by an REAC award from the University of California, San Francisco, and National Institutes of Health grant AR051077 (to YU).

Yoshikazu Uchida[1,2], Yunhi Cho[1,2,3], Sam Moradian[1,2], Jungmin Kim[1,2,3], Kimiko Nakajima[4], Debra Crumrine[1,2], Kyungho Park[1,2], Mayumi Ujihara[4], Masashi Akiyama[5], Hiroshi Shimizu[5], Walter M. Holleran[1,2,6], Shigetoshi Sano[4] and Peter M. Elias[1,2]

[1]Department of Dermatology, School of Medicine, University of California, San Francisco, San Francisco, California, USA; [2]Department of Veterans Affairs Medical Center and Northern California Institute for Research and Education, San Francisco, California, USA; [3]Department of Medical Nutrition, Graduate School of East-West Medical Science, Kyung Hee University, Seoul, South Korea; [4]Department of Dermatology, Kochi Medical School, Kochi University, Nankoku, Japan; [5]Department of Dermatology, Hokkaido University Graduate School of Medicine, Sapporo, Japan and [6]Department of Pharmaceutical Chemistry, School of Pharmacy, University of California, San Francisco, San Francisco, California, USA
E-mail: uchiday@derm.ucsf.edu

SUPPLEMENTARY MATERIAL

Supplementary material is linked to the online version of the paper at http://www.nature.com/jid

REFERENCES

Akiyama M, Sakai K, Takayama C *et al.* (2008) CGI-58 is an alpha/beta-hydrolase within lipid transporting lamellar granules of differentiated keratinocytes. *Am J Pathol* 173:1349–60

Behne M, Uchida Y, Seki T *et al.* (2000) Omega-hydroxyceramides are required for corneocyte lipid envelope (CLE) formation and normal epidermal permeability barrier function. *J Invest Dermatol* 114:185–92

Bouwstra JA, Gooris GS, Dubbelaar FE *et al.* (1998) Role of ceramide 1 in the molecular organization of the stratum corneum lipids. *J Lipid Res* 39:186–96

Demerjian M, Crumrine DA, Milstone LM *et al.* (2006) Barrier dysfunction and pathogenesis of neutral lipid storage disease with ichthyosis (Chanarin–Dorfman syndrome). *J Invest Dermatol* 126:2032–8

Elias PM, Williams ML (1985) Neutral lipid storage disease with ichthyosis. Defective lamellar body contents and intracellular dispersion. *Arch Dermatol* 121:1000–8

Elias PM, Williams ML, Holleran WM *et al.* (2008) Pathogenesis of permeability barrier abnormalities in the ichthyoses: inherited disorders of lipid metabolism. *J Lipid Res* 49:697–714

Radner FP, Streith IE, Schoiswohl G *et al.* (2009) Growth retardation, impaired triacylglycerol catabolism, hepatic steatosis, and lethal skin barrier defect in mice lacking comparative gene identification-58 (CGI-58). *J Biol Chem* 285:7300–11

Schweiger M, Lass A, Zimmermann R *et al.* (2009) Neutral lipid storage disease: genetic disorders caused by mutations in adipose triglyceride lipase/PNPLA2 or CGI-58/ABHD5. *Am J Physiol Endocrinol Metab* 297:E289–96

Stone SJ, Myers HM, Watkins SM *et al.* (2004) Lipopenia and skin barrier abnormalities in DGAT2-deficient mice. *J Biol Chem* 279:11767–76

Uchida Y, Behne M, Quiec D *et al.* (2001) Vitamin C stimulates sphingolipid production and markers of barrier formation in submerged human keratinocyte cultures. *J Invest Dermatol* 117:1307–13

Uchida Y, Holleran WM (2008) Omega-*O*-acylceramide, a lipid essential for mammalian survival. *J Dermatol Sci* 51:77–87

Ujihara M, Nakajima K, Yamamoto M *et al.* (2010) Epidermal triglyceride levels are correlated with severity of ichthyosis in Dorfman–Chanarin syndrome. *J Dermatol Sci* 57:102–7

Vasireddy V, Uchida Y, Salem Jr N *et al.* (2007) Loss of functional ELOVL4 depletes very long-chain fatty acids (>=C28) and the unique {omega}-*O*-acylceramides in skin leading to neonatal death. *Hum Mol Genet* 16:471–82

Wertz PW, Downing DT (1990) Metabolism of linoleic acid in porcine epidermis. *J Lipid Res* 31:1839–44

Yamaguchi T, Osumi T (2009) Chanarin-Dorfman syndrome: deficiency in CGI-58, a lipid droplet-bound coactivator of lipase. *Biochim Biophys Acta* 1791:519–23

Detection of Human Papillomavirus DNA in Plucked Eyebrow Hair from HIV-Infected Patients

Journal of Investigative Dermatology (2010) **130,** 2499–2502; doi:10.1038/jid.2010.147; published online 3 June 2010

TO THE EDITOR

The risk of developing human papillomavirus (HPV)-related benign and malignant cutaneous lesions is markedly increased in immunosuppressed people such as organ-transplant recipients (Harwood *et al.*, 2000) and HIV-infected patients (Grulich *et al.*, 2007; Stier and Baranoski, 2008). Although HPV DNA in plucked eyebrow hair has been well investigated (Boxman *et al.*, 1997) in renal transplant recipients and immunocompetent patients (ICPs) and correlated with both benign and malignant cutaneous lesions (Struijk *et al.*, 2003; Plasmeijer *et al.*, 2009), very little is known about HPV prevalence in eyebrow hair from HIV patients.

The study design was approved by the research ethics committee and all

Abbreviations: HPV, human papillomavirus; ICP, immunocompetent patient

Department of Health (AF0301). We thank Dr Michele Weiss for the figure illustration.

***Fred M. Kaplan*[1], *Michael J. Mastrangelo*[2,3] and *Andrew E. Aplin*[1,3]**

[1]Department of Cancer Biology, Thomas Jefferson University, Philadelphia, Pennsylvania, USA; [2]Department of Medical Oncology, Thomas Jefferson University, Philadelphia, Pennsylvania, USA and [3]Kimmel Cancer Center, Thomas Jefferson University, Philadelphia, Pennsylvania, USA
E-mail: Fred.Kaplan@mail.jc.tju.edu or Andrew.Aplin@KimmelCancerCenter.Org

REFERENCES

Davies H, Bignell GR, Cox C *et al.* (2002) Mutations of the BRAF gene in human cancer. *Nature* 417:949–54

Flaherty K, Puzanov I, Sosman J *et al.* (2009) Phase I study of PLX4032: proof of concept for V600E BRAF mutation as a therapeutic target in human cancer. *J Clin Oncol* 27: 15S (Abstract)

Halaban R, Zhang W, Bacchiocchi A *et al.* (2010) PLX4032, a selective BRAF V600E kinase inhibitor, activates the ERK pathway and enhances cell migration and proliferation of BRAF WT melanoma cells. *Pigment Cell Melanoma Res* 23: 190–200

Hall-Jackson CA, Eyers PA, Cohen P *et al.* (1999) Paradoxical activation of Raf by a novel Raf inhibitor. *Chem Biol* 6:559–68

Hatzivassiliou G, Song K, Yen I *et al.* (2010) RAF inhibitors prime wild-type RAF to activate the MAPK pathway and enhance growth. *Nature* 464:431–5

Heidorn SJ, Milagre C, Whittaker S *et al.* (2010) Kinase-dead BRAF and oncogenic RAS cooperate to drive tumor progression through CRAF. *Cell* 140:209–21

King AJ, Patrick DR, Batorsky RS *et al.* (2006) Demonstration of a genetic therapeutic index for tumors expressing oncogenic BRAF by the kinase inhibitor SB-590885. *Cancer Res* 66:11100–5

Michaloglou C, Vredeveld LC, Mooi WJ *et al.* (2008) BRAF(E600) in benign and malignant human tumours. *Oncogene* 27:877–95

Poulikakos PI, Zhang C, Bollag G *et al.* (2010) RAF inhibitors transactivate RAF dimers and ERK signalling in cells with wild-type BRAF. *Nature* 464:427–30

Ritt DA, Monson DM, Specht SI *et al.* (2010) Impact of feedback phosphorylation and Raf heterodimerization on normal and mutant B-Raf signaling. *Mol Cell Biol* 30:806–19

Rushworth LK, Hindley AD, O'Neill E *et al.* (2006) Regulation and role of Raf-1/B-Raf heterodimerization. *Mol Cell Biol* 26:2262–72

Tsai J, Lee JT, Wang W *et al.* (2008) Discovery of a selective inhibitor of oncogenic B-Raf kinase with potent antimelanoma activity. *Proc Natl Acad Sci USA* 105:3041–6

Complete Paternal Isodisomy of Chromosome 17 in Junctional Epidermolysis Bullosa with Pyloric Atresia

Journal of Investigative Dermatology (2010) **130,** 2671–2674; doi:10.1038/jid.2010.182; published online 1 July 2010

TO THE EDITOR

Uniparental disomy (UPD) is a condition in which two chromosomes of the same pair are inherited in whole or in part from only one parent. There are two types of UPD: uniparental isodisomy and uniparental heterodisomy. The former refers to two identical copies of a single homolog of a chromosome from one parent, and the latter indicates two different chromosome homologs from one parent. UPD can lead to an abnormal phenotype when isodisomy for a chromosome carrying a mutation for an autosomal-recessive disease gene results in homozygosity for the mutation.

Epidermolysis bullosa (EB) is a collection of heterogeneous disorders, in which congenital skin fragility leads to separation of the dermo-epidermal junction. EB has been subdivided into three major groups and one minor group, based on the level of blister formation: EB simplex, junctional EB, (JEB), dystrophic EB, and Kindler syndrome (Fine *et al.*, 2008). Mutations in 14 different genes have been identified as underlying EB subtypes (Fine *et al.*, 2008; Groves *et al.*, 2010). Among them, mutations in the gene encoding α6 integrin subunit (*ITGA6*) or β4 integrin subunit (*ITGB4*) are responsible for one rare subtype of JEB: JEB associated with pyloric atresia (JEB-PA). JEB-PA is inherited autosomal recessively and is characterized by generalized blistering and occlusion of the pylorus at birth, which usually leads to early demise. Most patients with JEB-PA have mutations in *ITGB4*, and more than 60 *ITGB4* mutations have been identified in JEB-PA cases.

The proband was the first child of nonconsanguineous healthy parents. There was no family history of bullous diseases. The child was born by cesarean section after a 35-week gestation because of polyhydramnion and had a birth weight of 1916 g and a birth length of 46.5 cm. Clinical manifestations of the proband included extensive blistering, especially on the extremities (Figure 1a). Routine abdominal X-ray demonstrated pyloric atresia (PA) (Figure 1b). No abnormalities other than skin fragility and PA were apparent. The proband died of sepsis 2 months after birth.

Immunofluorescence analysis revealed an absence of the β4 integrin subunit in skin specimens from the proband (Figure 1c–f). Expression of α6 integrin subunit and plectin was reduced in proband skin samples (Figure 1g and h). Immunostaining for BP230, laminin 332, and type VII collagen revealed normal linear-labeling patterns (Figure 1i–k).

Mutational analysis of all coding exons (exons 2–41) including the exon–intron boundaries of the *ITGB4* revealed that the proband was homozygous for c.953_955del in exon 8 (Figure 2a). The genomic DNA nucleotides, the

Abbreviations: EB, epidermolysis bullosa; JEB, junctional EB; JEB-PA, JEB with pyloric atresia; ITGA6, α6 integrin subunit; ITGB4, β4 integrin subunit; UPD, uniparental disomy

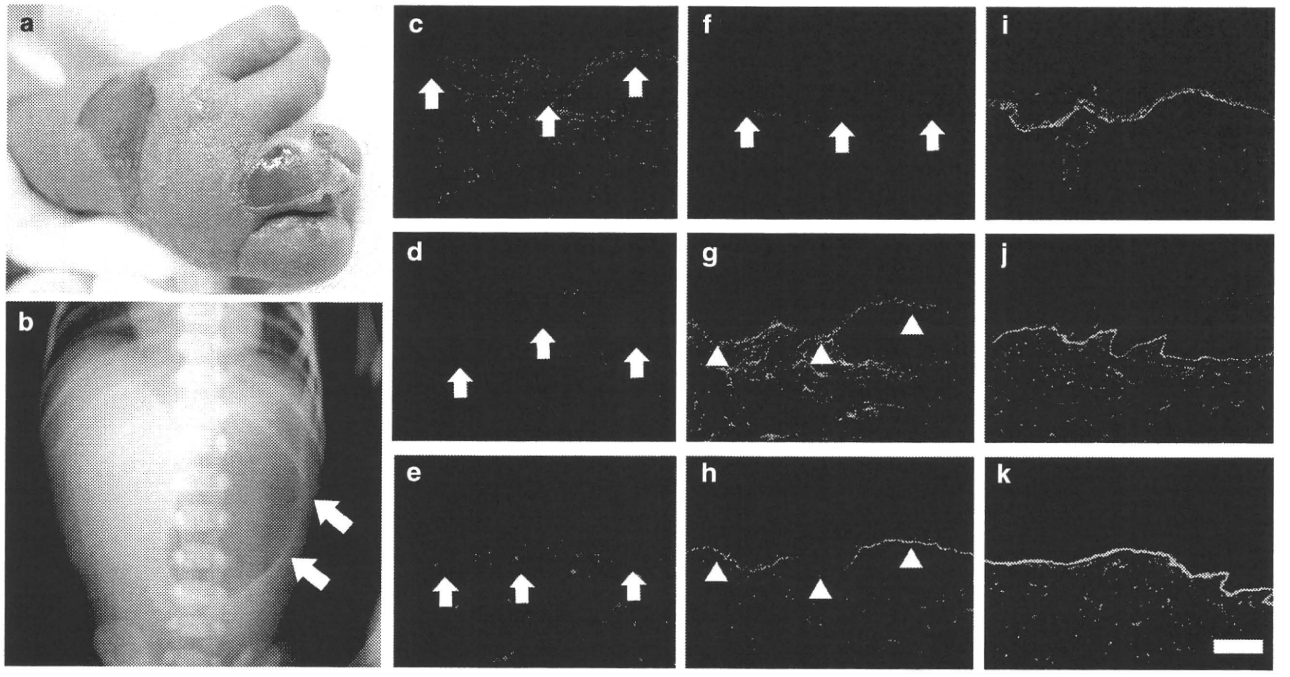

Figure 1. Clinical features of the proband and immunofluorescence analysis. (**a**) Extensive blistering is seen on the extremities at birth. (**b**) Abdominal X-ray reveals a single-bubble sign (arrows). β4 integrin subunit (3E1 (**c**), 113C (**d**), 450-9D (**e**), and 450-11A (**f**)) is not detected in the proband's skin (arrows). The expression of α6 integrin subunit (GoH3, **g**) and plectin (HD1-121, **h**) is diminished (arrowheads). BP230 (S1193, **i**), laminin-332 (GB3, **j**), and type VII collagen (LH7.2, **k**) show a normal linear staining pattern (scale bar = 100 μm). HD1-121 was donated by Professor Owaribe of Nagoya University, 113C by Professor Sonnenberg of the Netherlands Cancer Institute, 450-9D and 450-11A by Professor Lankford of the Oak Ridge National Laboratory, and S1193 by Professor Stanley of the University of Pennsylvania.

complementary DNA nucleotides and the amino acids of the protein were numbered based on the following sequence information (GenBank accession no. NM_000213). Mutation c.953_955del is predicted to result in the loss of asparagine at amino acid position 318 (p.Asn318del, Figure 2b), and this deletion mutation is not expected to cause subsequent frame-shift followed by a premature termination codon. Mutation c.953_955del was previously described in two JEB-PA cases (Iacovacci *et al.*, 2003; Varki *et al.*, 2006). The proband's father was heterozygous for this mutation (Figure 2a), although her mother revealed only normal sequences (Figure 2a).

To elucidate the origin of c.953_955del homozygosity in the proband, haplotype analysis of the entire chromosome 17 using 15 microsatellite markers (the ABI Prism Linkage Mapping Set Version 2.5 (Applied Biosystems, Warrington, UK)) was performed. The proband was found to be homozygous for all 15 microsatellite markers (Figure 2d). Ten of the 15 markers were fully informative for inheritance of two copies of a single paternal chromosome 17 in the proband (Figure 2d). For the non-chromosome 17 markers (D1S468, D1S252, D1S2842, D3S1297, D3S1566 and D3S1311), there were no discrepancies in the segregation of maternal and paternal alleles to the proband, confirming that the mother is indeed the biological mother of the patient (data not shown). Normal karyotyping ruled out monosomy of chromosome 17. The results in this family are compatible with the inheritance of two identical copies of a single chromosome 17 from the proband's father, which indicates complete paternal isodisomy of chromosome 17 in the proband. The medical ethical committee of Hokkaido University approved all the described studies. The study was conducted according to the Declaration of Helsinki Principles. Participants gave their written informed consent.

A recent review of the literature on UPD summarized 197 maternal and 68 paternal cases of UPD (Kotzot and Utermann, 2005). For UPDs of chromosome 17, only a few cases of maternal heterodisomy have been described (Genuardi *et al.*, 1999; Rio *et al.*, 2001). Recently, UPD of the whole chromosome 17 was reported as maternal heterodisomy of 17q and proximal 17p, and isodisomy of distal 17p (Lebre *et al.*, 2009). As far as we know, uniparental isodisomy of the whole chromosome 17 has not been described in the literature.

More than 35 cases of recessive-inherited disease have been reported as being caused by UPD (Kotzot and Utermann, 2005). UPD has been reported to be responsible for several EB subtypes, including Herlitz JEB (Castori *et al.*, 2008; Fassihi *et al.*, 2005; Pulkkinen *et al.*, 1997; Takizawa *et al.*, 2000; Takizawa *et al.*, 1998), EB simplex with pyloric atresia (Nakamura *et al.*, 2005) and recessive dystrophic EB (Fassihi *et al.*, 2006). So far, JEB-PA has not been described to result from UPD.

p.Asn318del (c.953_955del) has been identified as responsible for JEB-PA in two reports (Iacovacci *et al.*, 2003; Varki *et al.*, 2006). Asn^{318} in β4 integrin subunit resides in the extracellular

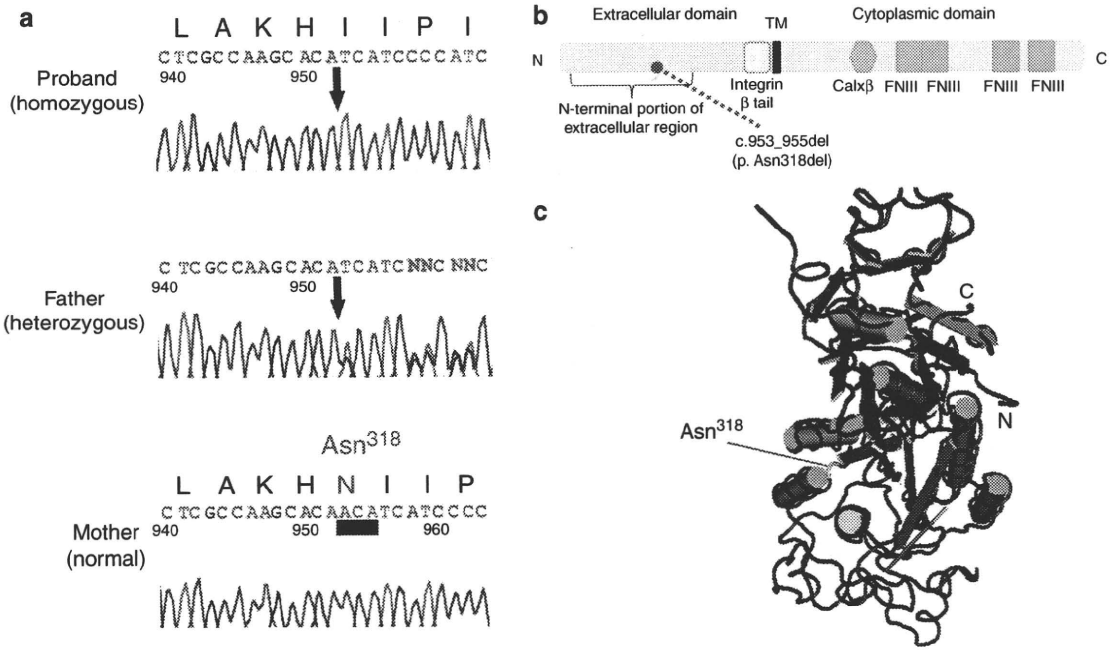

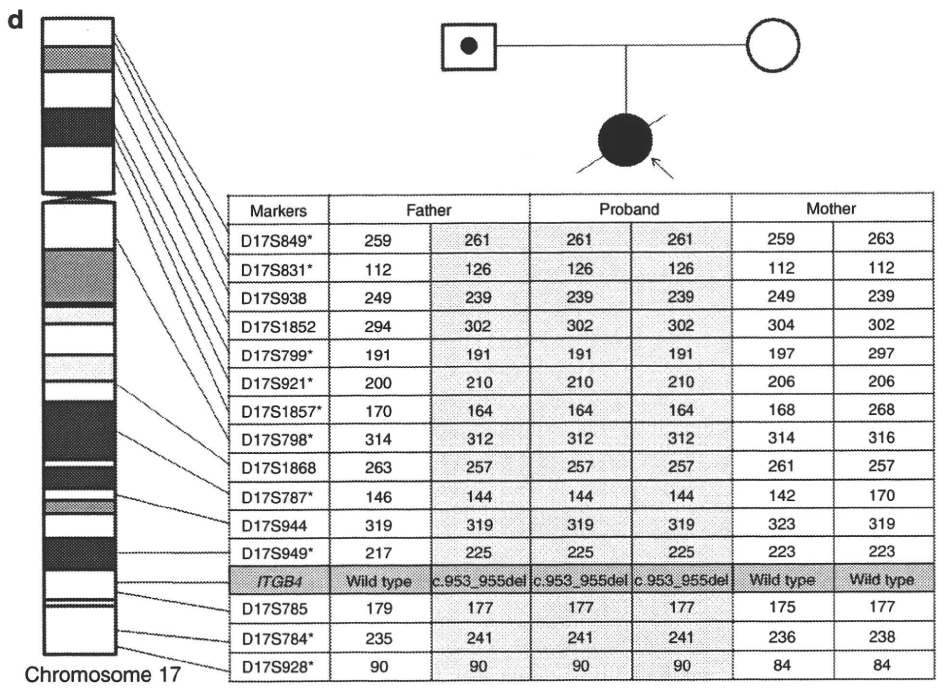

Markers	Father		Proband		Mother	
D17S849*	259	261	261	261	259	263
D17S831*	112	126	126	126	112	112
D17S938	249	239	239	239	249	239
D17S1852	294	302	302	302	304	302
D17S799*	191	191	191	191	197	297
D17S921*	200	210	210	210	206	206
D17S1857*	170	164	164	164	168	268
D17S798*	314	312	312	312	314	316
D17S1868	263	257	257	257	261	257
D17S787*	146	144	144	144	142	170
D17S944	319	319	319	319	323	319
D17S949*	217	225	225	225	223	223
ITGB4	Wild type	c.953_955del	c.953_955del	c.953_955del	Wild type	Wild type
D17S785	179	177	177	177	175	177
D17S784*	235	241	241	241	236	238
D17S928*	90	90	90	90	84	84

Figure 2. *ITGB4* mutation analysis. (**a**) The proband is homozygous for c.953_955 del (arrow). The proband's father is heterozygous for c.953_955 del (arrow). In contrast, the mother's gDNA shows only wild-type sequences. Deleted nucleotides are underlined. (**b**) Schematic arrangement of β4 integrin subunit and the positions of the mutation in the proband. (**c**) 3D imaging of the N-terminal extracellular domain of the integrin β chain (NCBI Conserved Domain Database (code: smart00187)) was done using Cn3D-4.1 software. Asn^{318} is in the linking loop between the α helix and the β sheet (arrow). (**d**) The proband was homozygous for all 15 microsatellite markers spanning all of chromosome 17. Ten of the 15 markers (*) suggest that the proband's alleles originated from one homolog of paternal chromosome 17.

domain of the protein (Figure 2b). This asparagine residue is an amino acid that is conserved not only in the β4 integrin subunit of vertebrates but in all the human integrin-β chains (Iacovacci *et al.*, 2003). The 3D structure of the N-terminal portion of the extracellular domain indicates that Asn^{318} consists of a linking loop between the α helix and the β sheet (Figure 2c). It is possible that the loss of this asparagine in the extracellular domain leads to significant conformational change and protein instability.

In summary, to our knowledge, we have reported the first case of complete